PLOS ONE

Oxidative/nitrative stress and inflammation drive progression of doxorubicin-induced renal fibrosis in rats as revealed by comparing a normal and a fibrosis-resistant rat strain

--Manuscript Draft--

Manuscript Number:	PONE-D-14-55246R1
Article Type:	Research Article
Full Title:	Oxidative/nitrative stress and inflammation drive progression of doxorubicin-induced renal fibrosis in rats as revealed by comparing a normal and a fibrosis-resistant rat strain
Short Title:	Oxidative stress in renal fibrosis resistance
Corresponding Author:	Peter Hamar, MD, PhD, Dsc Semmelweis University Budapest, Igen HUNGARY
Keywords:	renal fibrosis; Podocyte; Oxidative Stress; rat
Abstract:	Chronic renal fibrosis is the final common pathway of end stage renal disease caused by glomerular or tubular pathologies. Genetic background has a strong influence on the progression of chronic renal fibrosis. We recently found that Rowett black hooded rats were resistant to renal fibrosis. We aimed to investigate the role of sustained inflammation and oxidative/nitrative stress in renal fibrosis progression using this new model. Our previous data suggested the involvement of podocytes, thus we investigated renal fibrosis initiated by doxorubicin-induced (5 mg/kg) podocyte damage. Doxorubicin induced progressive glomerular sclerosis followed by increasing proteinuria and reduced bodyweight gain in fibrosis-sensitive, Charles Dawley rats during an 8-week long observation period. In comparison, the fibrosis-resistant, Rowett black hooded rats had longer survival, milder proteinuria and reduced tubular damage as assessed by neutrophil gelatinase-associated lipocalin (NGAL) excretion, reduced loss of the slit diaphragm protein, nephrin, less glomerulosclerosis, tubulointerstitial fibrosis and matrix deposition assessed by periodic acid-Schiff, Picro-Sirius-red staining and fibronectin immunostaining. Less fibrosis was associated with reduced profibrotic transforming growth factor-beta, (TGF-β1) connective tissue growth factor (CTGF), and collagen type I alpha 1 (COL-1a1) mRNA levels. Milder inflammation demonstrated by histology was confirmed by less monocyte chemotactic protein 1 (MCP-1) mRNA. As a consequence of less inflammation, less oxidative and nitrative stress was obvious by less neutrophil cytosolic factor 1 (p47phox) and NADPH oxidase-2 (p91phox) mRNA. Reduced oxidative enzyme expression was accompanied by less lipid peroxidation as demonstrated by 4-hydroxynonenal (HNE) and less protein nitrosylation demonstrated by nitrotyrosine (NT) immunohistochemistry and quantified by Western blot. Our results demonstrate that mediators of fibrosis, inflammation and oxidative/nitrative stress were suppressed in doxorubicin nephropathy in fibrosis-resistant Rowett black hooded rats underlying the importance of these pathomechanisms in the progression of renal fibrosis initiated by glomerular podocyte damage.
Order of Authors:	Csaba Imre Szalay
	Katalin Erdélyi
	Gábor Kökény
	Enikő Lajtár
	Mária Godó
	Csaba Révész
	Tamás Kaucsár
	Norbert Kiss
	Márta Sárközy

	Tamás Bálint Csont
	Tibor Krenács
	Gábor Szénási
	Pál Pacher
	Peter Hamar, MD, PhD, Dsc
Opposed Reviewers:	
Response to Reviewers:	Review Comments to the Author Reviewer #1: The paper is well written and the data are interesting. Resistance against the development of fibrosis is an interesting field of research. The major flaw of this paper however is that the authors are looking at resistance against the response to ADR. Proteinuria in ADR nephrosis is induced by damage to the podocytes. Proteinuria subsequently drives renal changes and if the BH rat is resistant against fibrosis the authors should also use a group of animals in which the proteinuria is similar as in the control groups. If the BH rat is resistant against fibrosis it schooled develop less fibrosis while having the same level of proteinuria. Answer: This is an excellent suggestion, thank you! In order to investigate tubulointerstitial fibrosis development in the resistant BH rats with similar extent of proteinuria, we selected ADR (DXR)-treated CD (CD/DXRp) and BH (BH/DXRp) subgroups with matched protein excretion. The majority of fibrosis and oxidative stress markers were significantly lower in the resistant BH/DXRp rats in comparison to those in CD/DXRp group, despite a small number of animals (n=4 or 5) in these subgroups. We include these results now in the revised version of the manuscript. We hope that the substantial differences between the two subgroups despite the small sample size sufficiently support our conclusion that the BH strain is resistant not only to glomerular ADR injury and chronic fibrotic renal damage in general but also to tubulointerstitial fibrosis developing as a consequence of proteinuria. Reviewer #2: This is an interesting paper from an experienced laboratory. The authors provide convincing evidence that oxidative/nitrative stress and inflammation associate with doxorubicin-induced renal fibrosis in rats. The experiments are well designed and appear to be carefully conducted. The results are sound and the manuscript is well-written. Reviewer #3: PONE-D-14-55246 : Oxidative/nitrative stress and inflammation drive progression of doxorubicin-induced renal fibrosis in rats as revealed by comparing a normal and a fibrosis-resistant rat strain. The authors investigated the role of sustained inflammation and oxidative stress in renal fibrosis progression using a doxorubicin-induced fibrosis rat model. After comparing levels of a number of factors and markers of fibrosis and oxidative stress in two rat strains (resistant and susceptible), the authors concluded that mediators of fibrosis, inflammation and oxidative stress were suppressed in fibrosis-resistant Rowett black hooded rats. The paper raised some of the following suggestions and concerns. 1.Methods used in the study are described in excessive details, would be beneficial to omit redundant details which are parts of standard procedures and are not specific for the described experiments. Paragraphs “Animals and experimental design “and “Survival experiment” should be combined into 1 paragraph, the same should be done for histochemistry stainings. It is not clear why the authors selected the dilutions for urine samples in “103-105 fold” range for the NGAL assay. Answer: Thank you for pointing these out! We shortened the “Materials and methods” section substantially, including your suggestions to combine the survival experiments and histochemistry into previous paragraphs. The “103-105 fold” part was a text formatting error. The samples were diluted 103-105 times (1000-100000) based on the manufacturer’s instructions and our previous experience. We corrected this mistake in the revised manuscript. 2. The paragraph on absence of heart toxicity and corresponding figure 1 panels seem excessive considering the title.

Answer: Numerous studies use small repeated doses of Doxorubicin to model hearth failure in rats. We wanted to convincingly exclude cardiomyopathy in BH and CD rats in our experiment. Certainly, the aim was to study renal function and not heart toxicity, so we shortened the paragraph on absence of heart toxicity, and omitted the figure from the revised manuscript.

3. The discussion lists references with not always relevant content. For example: “We present here an animal model useful to investigate the pathomechanisms of hereditary susceptibility or resistance to renal fibrosis [10,33,34]”. Of the 3 references only #34 is related to DOX model presented in the paper, while 2 others are on HIVAN and diabetic nephropathy.
Also, the authors mentioned that doxorubicin-induced nephropathy (DOXN) was studied in mice and cite references which report initial stages of the study, but not the paper which reported the final finding: in the mouse model susceptibility to DOXN was caused by a mutation in Prkdc gene, which has well-established function in DNA repair. Even more, the authors wrote: “The susceptibility of BALB/c mice against DXR nephropathy was associated with a gene involved in DXR detoxification. In this study C57BL/6 mice - generally resistant to renal fibrosis - were compared to sensitive Balb/c mice with known differences in inflammatory response. C57Bl/6 mice are typically Th1 predominant, vs. Th2 529 predominance in BALB/c mice [58]”. It is surprising, as the referenced (#58) paper discusses only innate immunity response in BALB/c and C57BL/6 strains.

Answer: Thank you for pointing out these issues. We cited references 10, 33, 34 to emphasize the role of genetic background in susceptibility to renal fibrosis in general; therefore we cited various kidney injury models. Now we rephrased the sentence to make this aim clear.
The references for different sensitivity of C57BL/6 and BALB/c mice and the PRKDC study are now cited as you suggested. The Watanabe paper (#59 in the revised manuscript) discusses indeed innate immune response in BALB/c and C57BL/6 mice, but summarizes substantial evidence supporting that “C57BL/6 and BALB/c mice are prototypical Th1- and Th2-type mouse strains, respectively.” However, as we have no direct evidence in favor of the Th1/Th2 paradigm, we deleted this part from the revised manuscript.

4. It would be interesting to know if the mutations in Prkdc were checked in the rat strains studied here.

Answer: We agree that it would be very interesting to know the PRKDC status in the two strains studied. As the Rowett Black Hooded (BH) rat is primarily used as a background strain for the Rowett Nude (RNU) – thymus deficient rat, we could not find any literature on the PRKDC status of this strain. Also for the search terms: “prkdc + rat” and “DNA-PK gene + rat” we found only 22 and 7 PubMed hits, respectively – none of them used the rat strains of our study. However, we extended the discussion of the revised manuscript on the potential role of DNA repair.

5. The authors measured levels of a number of inflammation factors, oxidative stress and fibrosis markers using qPCR and IHC. The work seems purely descriptive and applies previously published data to the comparison of the two rat strains with different degree of susceptibility to DOXN. It would make the paper more interesting if the authors presented their view on the underlying mechanism and discussion of the primary and secondary nature of measured differences and changes related to the severity of DOX-induced fibrosis in the compared strains

Answer: It is tempting to define the underlying mechanism(s) of resistance against the DOX-induced nephropathy (DOXN) in the BH strain. We speculate that the initial toxic injury of DOX induces podocyte damage and consequent albuminuria. Albumin (and possibly DOX) cause tubular injury inducing inflammation. Inflammation is accompanied by oxidative stress, inducing further inflammation. The vicious cycle of chronic inflammation manifests as fibrosis. The resistant BH strain is protected by a more mild inflammatory reaction and softer oxidative damage. We aimed to summarize this in Fig. 6. We believe that in such a vicious circle, causes and consequences are hard to separate as damage induces inflammation, which induces further (oxidative)

	damage. We aimed to symbolize these vicious circles by the thick round arrows pointing back to earlier steps in Fig. 6. We extended the legend of Fig. 6 to make this point clearer.
Additional Information:	
Question	**Response**
Financial Disclosure Please describe all sources of funding that have supported your work. A complete funding statement should do the following: Include **grant numbers and the URLs** of any funder's website. Use the full name, not acronyms, of funding institutions, and use initials to identify authors who received the funding. **Describe the role** of any sponsors or funders in the study design, data collection and analysis, decision to publish, or preparation of the manuscript. If they had no role in any of the above, include this sentence at the end of your statement: "*The funders had no role in study design, data collection and analysis, decision to publish, or preparation of the manuscript.*" If the study was **unfunded**, provide a statement that clearly indicates this, for example: "*The author(s) received no specific funding for this work.*" * typeset	Support was provided to P. Hamar from the Hungarian Research Fund: OTKA K81972, NF69278, K110810, ETT 07-011/ 2009, and to P. Pacher from the Intramural Research Program of NIAAA/NIH. P Hamar acknowledges support from the Bolyai Research Scholarship of the Hungarian Academy of Sciences and the Merit Prize of the Semmelweis University.
Competing Interests You are responsible for recognizing and disclosing on behalf of all authors any competing interest that could be perceived to bias their work, acknowledging all financial support and any other relevant financial or non-financial competing interests. Do any authors of this manuscript have competing interests (as described in the PLOS Policy on Declaration and Evaluation of Competing Interests)? **If yes**, please provide details about any and all competing interests in the box below. Your response should begin with	None

this statement: *I have read the journal's policy and the authors of this manuscript have the following competing interests:* **If no** authors have any competing interests to declare, please enter this statement in the box: "*The authors have declared that no competing interests exist.*" * typeset	
Ethics Statement You must provide an ethics statement if your study involved human participants, specimens or tissue samples, or vertebrate animals, embryos or tissues. All information entered here should **also be included in the Methods section** of your manuscript. Please write "N/A" if your study does not require an ethics statement. **Human Subject Research (involved human participants and/or tissue)** All research involving human participants must have been approved by the authors' Institutional Review Board (IRB) or an equivalent committee, and all clinical investigation must have been conducted according to the principles expressed in the Declaration of Helsinki. Informed consent, written or oral, should also have been obtained from the participants. If no consent was given, the reason must be explained (e.g. the data were analyzed anonymously) and reported. The form of consent (written/oral), or reason for lack of consent, should be indicated in the Methods section of your manuscript. Please enter the name of the IRB or Ethics Committee that approved this study in the space below. Include the approval number and/or a statement indicating approval of this research. **Animal Research (involved vertebrate animals, embryos or tissues)** All animal work must have been conducted according to relevant national	Humane endpoints were used to minimize suffering in survival studies. Animals were observed and weighed every morning after potentially lethal interventions including DXR administration. If clinical signs of distress were recognized the animals were euthanized by cervical dislocation performed by a trained personnel. Clinical signs of renal failure are described in the methods of survival study. Uremic signs or body weight loss exceeding 40% of the initial body-weight was an indication for euthanasia. Sacrifice for organ removal was performed under ketamine (CP-Ketamin 10%, CP-Pharma, Burgdorf, Germany) + xylazin (CP-Xylazin 2%, CP-Pharma, Burgdorf, Germany) anesthesia. All procedures were performed in accordance with guidelines set by the National Institutes of Health and the Hungarian law on animal care and protection. The experimental protocol was reviewed and approved by the “Institutional Ethical Committee for Animal Care and Use” of Semmelweis University (registration number: XIV-I-001/2104-4/2012).

and international guidelines. If your study involved non-human primates, you must provide details regarding animal welfare and steps taken to ameliorate suffering; this is in accordance with the recommendations of the Weatherall report, "The use of non-human primates in research." The relevant guidelines followed and the committee that approved the study should be identified in the ethics statement. If anesthesia, euthanasia or any kind of animal sacrifice is part of the study, please include briefly in your statement which substances and/or methods were applied. Please enter the name of your Institutional Animal Care and Use Committee (IACUC) or other relevant ethics board, and indicate whether they approved this research or granted a formal waiver of ethical approval. Also include an approval number if one was obtained. **Field Permit** Please indicate the name of the institution or the relevant body that granted permission.	
Data Availability PLOS journals require authors to make all data underlying the findings described in their manuscript fully available, without restriction and from the time of publication, with only rare exceptions to address legal and ethical concerns (see the PLOS Data Policy and FAQ for further details). When submitting a manuscript, authors must provide a Data Availability Statement that describes where the data underlying their manuscript can be found. Your answers to the following constitute your statement about data availability and will be included with the article in the event of publication. **Please note that simply stating 'data available on request from the author' is not acceptable.** ***If, however, your data are only available upon request from the author(s), you must answer "No" to the first question below, and explain your exceptional situation in the text box provided.*** Do the authors confirm that all data	Yes - all data are fully available without restriction

underlying the findings described in their manuscript are fully available without restriction?	
Please describe where your data may be found, writing in full sentences. **Your answers should be entered into the box below and will be published in the form you provide them, if your manuscript is accepted.** If you are copying our sample text below, please ensure you replace any instances of XXX with the appropriate details. If your data are all contained within the paper and/or Supporting Information files, please state this in your answer below. For example, “All relevant data are within the paper and its Supporting Information files.” If your data are held or will be held in a public repository, include URLs, accession numbers or DOIs. For example, “All XXX files are available from the XXX database (accession number(s) XXX, XXX)." If this information will only be available after acceptance, please indicate this by ticking the box below. If neither of these applies but you are able to provide details of access elsewhere, with or without limitations, please do so in the box below. For example: “Data are available from the XXX Institutional Data Access / Ethics Committee for researchers who meet the criteria for access to confidential data.” “Data are from the XXX study whose authors may be contacted at XXX.” * typeset	Data of the current study are available from Péter Hamar the corresponding author, who may be contacted at hamar.peter@med.semmelweis-univ.hu.
Additional data availability information:	

From: Dr. Péter Hamar, MD, PhD, DSc Budapest, 18/03/2015

Institute of Pathophysiology,
Semmelweis University,
4. Nagyvárad tér
Budapest, 1089
Hungary

To: Dr. Damian Pattinson
Editorial Director,
PLOS ONE

Dear Dr. Pattinson,

Please find attached our revised manuscript entitled "Oxidative/nitrative stress and inflammation drive progression of doxorubicin induced renal fibrosis in rats as revealed by comparing a normal and a fibrosis resistant rat strain" - PONE-D-14-55246R1.

The manuscript was revised according to the critique of the reviewers. We really appreciate the helpful comments of the reviewers. We accepted all suggestions made by the referees. We believe that the changes made to the manuscript based on the referees' suggestions substantially improved the manuscript and made its message clearer.

May I assure you that we would be very pleased and honoured if you found our revised manuscript suitable for publication in Plos One?

Yours sincerely,

Péter Hamar
for the authors

Oxidative/nitrative stress and inflammation drive progression of doxorubicin-induced renal fibrosis in rats as revealed by comparing a normal and a fibrosis-resistant rat strain

Authors: Csaba Imre Szalay[1], Katalin Erdelyi[2], Gábor Kökény[1], Enikő Lajtár[1], Mária Godó[1], Csaba Révész[1], Tamás Kaucsár[1], Norbert Kiss[1], Márta Sárközy[3], Tamás Csont[3], Tibor Krenács[4], Gábor Szénási[1], Pál Pacher[2¶], Péter Hamar[1¶*]

Affiliations:

[1] Semmelweis University, Institute of Pathophysiology, Budapest, Hungary

[2] National Institute of Health (NIH/NIAAA/DICBR), Laboratory of Physiological Studies, Section on Oxidative Stress and Tissue Injury, Bethesda, MD, USA

[3] University of Szeged, Faculty of Medicine, Department of Biochemistry, Szeged, Hungary

[4] 1st Semmelweis University, Department of Pathology and Experimental Cancer Research; MTA-SE Tumor Progression Research Group, Budapest, Hungary

* Corresponding author

E-mail: hamar.peter@med.semmelweis-univ.hu (PH)

¶: These authors contributed equally to this work.

Short title: Oxidative stress in renal fibrosis resistance

Key words: renal fibrosis, podocyte, oxidative stress, rat

List of abbreviations:

BH: black hooded, Rowett rats

BH/c or CD/c: control rats (injected with Saline)

BH/DXR or CD/DXR: doxorubicin-injected rats

CD: Charles Dawley rats

CKD: chronic kidney disease

COL1A1: collagen type I alpha 1

Ct: cycle time

CTGF: connective tissue growth factor

DXR: doxorubicin

FSGS: focal segmental glomerulosclerosis

HNE: 4-hydroxy-2-nonenal

IFTA: Interstitial fibrosis and tubular atrophy

MCP-1: monocyte chemotactic protein 1

mRNA: messenger ribonucleic acid

NGAL: neutrophil gelatinase-associated lipocalin

NOX: nicotinamide adenine dinucleotide phosphate-oxidase

NT: nitrotyrosine

$p47^{phox}$: neutrophil cytosolic factor 1 (Ncf1), neutrophil NOX-2 subunit

$p91^{phox}$: NOX-2, cytochrome b-245 beta polypeptide, neutrophil NOX-2 subunit

Phox: Phagocyte oxidase

RT-qPCR: reverse transcription - quantitative polymerase chain reaction

ROS: reactive oxygen species

SHR: spontaneously hypertensive rats

48 TGF-β1: transforming growth factor β1

49

Abstract (word count: 294)

Chronic renal fibrosis is the final common pathway of end stage renal disease caused by glomerular or tubular pathologies. Genetic background has a strong influence on the progression of chronic renal fibrosis. We recently found that Rowett black hooded rats were resistant to renal fibrosis. We aimed to investigate the role of sustained inflammation and oxidative/nitrative stress in renal fibrosis progression using this new model. Our previous data suggested the involvement of podocytes, thus we investigated renal fibrosis initiated by doxorubicin-induced (5 mg/kg) podocyte damage. Doxorubicin induced progressive glomerular sclerosis followed by increasing proteinuria and reduced bodyweight gain in fibrosis-sensitive, Charles Dawley rats during an 8-week long observation period. In comparison, the fibrosis-resistant, Rowett black hooded rats had longer survival, milder proteinuria and reduced tubular damage as assessed by neutrophil gelatinase-associated lipocalin (NGAL) excretion, reduced loss of the slit diaphragm protein, nephrin, less glomerulosclerosis, tubulointerstitial fibrosis and matrix deposition assessed by periodic acid–Schiff, Picro-Sirius-red staining and fibronectin immunostaining. Less fibrosis was associated with reduced profibrotic transforming growth factor-beta, (TGF-β1) connective tissue growth factor (CTGF), and collagen type I alpha 1 (COL-1a1) mRNA levels. Milder inflammation demonstrated by histology was confirmed by less monocyte chemotactic protein 1 (MCP-1) mRNA. As a consequence of less inflammation, less oxidative and nitrative stress was obvious by less neutrophil cytosolic factor 1 ($p47^{phox}$) and NADPH oxidase-2 ($p91^{phox}$) mRNA. Reduced oxidative enzyme expression was accompanied by less lipid peroxidation as demonstrated by 4-hydroxynonenal (HNE) and less protein nitrosylation

demonstrated by nitrotyrosine (NT) immunohistochemistry and quantified by Western blot. Our results demonstrate that mediators of fibrosis, inflammation and oxidative/nitrative stress were suppressed in doxorubicin nephropathy in fibrosis-resistant Rowett black hooded rats underlying the importance of these pathomechanisms in the progression of renal fibrosis initiated by glomerular podocyte damage.

Introduction:

Chronic kidney disease (CKD) is a major healthcare problem with a prevalence of 7% in Europe [1], and over 10% in the US according to the Centers for Disease Control and Prevention [2]. The pathologic manifestation of CKD is renal fibrosis, which is the final common pathway of many kidney diseases, such as diabetic and hypertensive nephropathy, toxic, ischemic or autoimmune renal diseases [3,4].

The clinical presentation of CKD varies widely among patients with the same initial disease [5]. The severity of symptoms and the rate of CKD progression are influenced by age, gender [6,7] and numerous pieces of evidence support a role for genetic background in progression [8,9,10]. We have demonstrated previously that Rowett, black hooded (BH) rats were resistant to renal fibrosis induced by subtotal nephrectomy plus salt and protein loading [11]. Better understanding of such resistance can shed light on the pathomechanisms of fibrosis in general and renal fibrosis specifically.

The anthracycline derivative chemotherapeutic drug, Doxorubicin (Adriamycin, DXR) is widely used as a rodent model of proteinuric nephropathy leading to renal fibrosis [12]. Although it is generally accepted that an initial injury to podocytes induces proteinuria, the exact pathomechanism of the DXR-induced nephropathy is poorly understood [13]. The role of sustained inflammation and oxidative stress has been demonstrated in many experimental models of renal fibrosis, including the remnant kidney [11,14,15] and DXR nephropathy models [12,16,17,18,19]. The myocardial and renal side effects of DXR are mainly attributed to the generation of free oxygen radicals [20]. DXR exerts direct toxic damage to the glomerular structure leading to loss of nephrin [21] and consequent proteinuria [22]. Proteinuria per se, sustained

inflammation and accompanying oxidative damage are major mechanisms of progressive renal fibrosis [12]. It has been reported that the DXR-induced oxidative damage in cells of the renal cortex paralleled renal fibrosis progression [23]. DXR administration to rats led to severe tubulointerstitial inflammation with marked infiltration by T and B lymphocytes and macrophages. The intensity of inflammation correlated with the DXR-induced renal damage, and modifying pro-inflammatory pathways affected the severity of renal damage in this model [24,25,26].

We hypothesized that milder inflammation and milder accompanying oxidative/nitrative stress may be responsible for the previously published resistance of BH rats to renal fibrosis. To investigate the role of oxidative/nitrative stress and inflammation in the BH rats' protection from renal fibrosis, we compared CD and BH rats in DXR nephropathy model.

Materials and Methods

Ethics Statement

Humane endpoints were used to minimize suffering in survival studies. Animals were observed and weighed every morning after potentially lethal interventions including DXR administration. If clinical signs of distress were recognized the animals were euthanized by cervical dislocation performed by a trained personnel. Uremic signs or body weight loss > 40% of the initial body-weight was an indication for euthanasia. Clinical signs of uremia are described later. Sacrifice for organ removal was performed under ketamine + xylazin (CP-Ketamin 10%, CP-Xylazin 2%, CP-Pharma, Burgdorf, Germany) anesthesia. All procedures were performed in accordance with guidelines set by the National Institutes of Health and the Hungarian law on animal

care and protection. The experimental protocol was reviewed and approved by the "Institutional Ethical Committee for Animal Care and Use" of Semmelweis University (registration number: XIV-I-001/2104-4/2012).

Animals and experimental design

Eight-week-old male Charles Dawley (CD) and Rowett, black hooded (BH) rats were used in the studies (Charles River, Hungary). After arrival the animals were allowed 1 week for acclimatization. All animals were maintained under standardized (light on 08:00–20:00 h; 40–70% relative humidity, 22±1°C), specified pathogen-free (SPF) conditions, with free access to water and standard rodent chow (Altromin standard diet, Germany).

We performed the following three experiments:

1. Renal functional and morphological experiment in DXR-induced acute renal failure;
2. Long term survival study with low dose DXR;
3. Short term survival study with high dose DXR.

In the functional and morphological experiment (exp. 1) rats (n=8/group) were intravenously injected with 5 mg/kg body weight DXR (Sicor S.r.l. Società Italiana Corticosteroidi, Italy) dissolved in saline. Equal volume of saline was administered to control animals. DXR dose was based on literature data and pilot experiments. In the pilot experiments 2 mg/kg DXR did not induce renal damage, whereas 8 mg/kg DXR caused premature moribund state in some animals. Urinary protein and NGAL excretion was followed for 8 weeks when the experiment was terminated and renal morphology was investigated. Long-term survival (exp. 2) was evaluated in age

matched BH and CD rats (n=8/group) (5 mg/kg DXR, iv). For short-term survival (exp. 3) 10 mg/kg DXR was injected iv (n=8/group). In survival experiments animals were euthanized upon signs of uremia, which included reduced locomotion, pilo-erection, body weight loss or dyspnoea. Blood urea was > 250 mg/dl in each euthanized animal demonstrating that uremia was the cause of the moribund state.

In order to investigate whether the difference in the degree of tubulointerstitial fibrosis between the two rat strains was the consequence of different tubular protein load, or BH rats were resistant to tubulointerstitial fibrosis per se, we formed two sub-groups. In this analysis CD and BH rats treated with DXR (CD/DXRp, n=4 and BH/DXRp, n=5) were matched for urinary protein excretion and sensitive molecular, inflammatory and fibrosis parameters were compared.

Proteinuria and NGAL excretion

Proteinuria was measured as a sensitive indicator of podocyte injury and progression of renal fibrosis. Urine was collected for 24 hours in diuresis cages (Techniplast, Italy) before (self-control) and biweekly after DXR administration. Urine protein concentration was assessed with a pyrogallol red colorimetric assay (Diagnosticum Ltd, Budapest, Hungary). Optical density was measured at 598 nm with the SpectraMax 340 Microplate Spectrophotometer (Molecular Devices, Sunnyvale, USA).

Urine NGAL levels were measured with rat Lipocalin-2/NGAL DuoSet ELISA Development kit (R&D Systems, USA) as described by the manufacturer. Optical density was measured with Victor3™ 1420 Multilabel Counter (PerkinElmer, WALLAC Oy, Finland) at 450 nm with wavelength correction set to 544 nm.

Concentrations were calculated with WorkOut (Dazdaq Ltd., England), using a four parameter logistic curve-fit.

Sacrifice and renal sample collection

In the functional and morphological study (exp. 1), rats were anesthetized with ketamine + xylazine 8 weeks after DXR administration. To prevent blood clotting, 1 ml/kg Na-EDTA (Sigma-Aldrich Corporation, Saint Louis, MO, USA) was injected intraperitoneally. Rats were bled from the aorto-femoral bifurcation. Animals were perfused through the aorta with 60 ml cold physiological saline to remove blood from the vasculature. After perfusion, the left kidney and the heart were removed and sectioned for further analysis. The heart and a third of the left kidney were fixed in 4% buffered formaldehyde and were later embedded in paraffin for basic histological and immunohistochemical analysis. The remaining two third of the left kidney cortex and medulla were separated, frozen in liquid nitrogen and stored at -80 °C for molecular studies.

Renal morphology

Glomerulosclerosis was assessed according to a modified [11,27] scoring system (scores 0–4) of El Nahas et al. [28] at x400 absolute magnification using an Olympus CX21 microscope (Olympus Optical Co. Ltd., Japan). Score 0: normal glomerulus. Score 1: thickening of the basal membrane. 2: mild (<25%), 2.5: severe segmental (>50%) and 3: diffuse hyalinosis. 4: total tuft obliteration and collapse. The glomerular score of each animal was derived as the arithmetic mean of 100 glomeruli.

Tubulointerstitial damage was assessed with a semi quantitative scale (magnification ×100) of percent area affected by tubulointerstitial changes [21,29]. Score 0: normal tubules and interstitium, 1: brush border loss or tubular dilatation in <25% of the field of view (fv). 2: tubular atrophy, dilation and casts in < 50% fv. Score 3: tubular and interstitial damage in < 75% fv, 4: tubular atrophy, dilation, casts and fibrosis > 75% fv. The overall score was the mean of 15 fvs.

Inflammatory infiltration was assessed on hematoxylin-eosin stained sections by the percent of area infiltrated by inflammatory cells (magnification: x400). Score 0: normal glomeruli, tubules and interstitium, 1: inflammatory cells present in <25% fv. 2: inflammation in < 50% fv. Score 3: inflammation in < 75% fv, 4: inflammation in > 75% of fv. The overall score was the mean of 120 fvs.

Collagen deposition in the renal interstitium was demonstrated by Picro-Sirius Red staining as described previously. Fibrotic areas were quantified using Image J software (National Institutes of Health, Bethesda, Maryland, US).

Antibodies

For Western blot and immunohistochemistry: 4-hydroxy-2-nonenal (HNE, mouse monoclonal, clone: HNEJ-2, JaICA, Japan), NT (mouse monoclonal, #189542, Cayman Chemical Company, Michigan, IL), fibronectin (rabbit polyclonal, Sigma-Aldrich, Budapest, Hungary), Connexin-43 (1:100, #3512, Cell Signaling, Beverly, MA) were used.

Western Blot

The kidney samples were lysed in RIPA Buffer (Thermo Scientific, Rockford, IL). Protein concentration was determined by the bicinchoninic acid (BCA) protein assay (Thermo Scientific, Rockford, IL). Twenty µg protein was resolved on 4-12% Criterion™ XT Bis-Tris Precast gels (BioRad, Hercules, CA) and transferred to nitrocellulose membrane to detect HNE or to Polyvinylidene Difluoride (PVDF) membrane to detect NT. The primary NT antibody was applied at 1.3 µg/mL and the primary HNE antibody at 0.3 µg/mL. The secondary antibody (peroxidase conjugated goat anti-mouse, PerkinElmer, Santa Clara, CA) was applied at 0.25 µg/mL. Blots were incubated in enhanced chemiluminescence substrate, Supersignal West Pico Chemiluminescent Substrate (Thermo Scientific, Rockford, IL), and were exposed to photographic film. After stripping membrane with Restore™ Western Blot Stripping Buffer (Thermo Scientific, Rockford, IL), as a loading control, peroxidase conjugated anti-actin (AC-15 Abcam, Cambridge, MA) was applied at 70 ng/mL concentration in blocking buffer for 1 h at room temperature.

Immunohistochemistry

Paraffin sections on Superfrost™ Ultra Plus Adhesion Slides (Thermo Fisher Scientific Inc, Waltham, MA, USA) were deparaffinized and rehydrated in ethanol. Fibronectin immunohistochemistry was performed with rabbit polyclonal anti-fibronectin antibody (1:2000, Sigma-Aldrich, Budapest, Hungary), using the avidin–biotin method [30]. HNE and NT immunohistochemistry was performed with mouse monoclonal antibody (HNE clone: HNEJ-2, JaICA, Japan; NT clone: #189542, Cayman Chemical Company, Michigan, IL). Color development was induced by incubation with diaminobenzidine (DAB) kit (Vector Laboratories, Burlingame, CA).

Pictures were taken from the stained sections for further analysis. The fibronectin stained area was quantified with Image J software.

Heart fibrosis markers

In a separate group, the hearts were removed and fixed in 4% buffered formalin and embedded similarly to the renal samples 8 weeks after 5 mg/kg DXR administration. Consecutive sections were stained with Masson's trichrome to detect collagen deposition as a sign of chronic fibrosis, and direct immunofluorescence was performed for connexin-43 (Cx43), an early marker of cardiomyocyte damage.

Monitoring mRNA levels with Real-Time quantitative Polymerase Chain Reaction (RT-qPCR)

RNA preparation

Total RNA for RT-qPCR was extracted by homogenizing 50-80 mg pieces of renal cortex in TRI Reagent® (Molecular Research Center Inc., Cat. NO.: TR118) according to the manufacturer's protocol. DNA contamination was removed by TURBO DNase (Life technologies, Ambion®, Cat. No: AM2238). RNA concentration and purity of the samples was measured with the NanoDrop 2000c Spectrophotometer (Thermo Fisher Scientific Inc, Waltham, MA, USA). The RNA integrity was verified by electrophoretic separation on 1% agarose gel.

RT-qPCR analysis of renal mRNA levels

Reverse transcription of 1 µg total renal RNA into cDNA was carried out using random hexamer primers and the High-Capacity cDNA Archive Kit (Applied

Biosystem™, USA) according to the manufacturer's protocol. Messenger RNA levels of NADPH oxidase-2 (NOX-2, $p91^{phox}$, cytochrome b-245 beta polypeptide), neutrophil cytosolic factor 1 (Ncf1, $p47^{phox}$), collagen type I, alpha 1 (COL1A1), transforming growth factor β1 (TGF-β1), connective tissue growth factor (CTGF) and macrophage chemotactic protein 1, (MCP-1, chemokine (C-C motif) ligand 2, Ccl2) were measured by RT-qPCR (Qiagen, Hilden, Germany) and target mRNA levels were normalized to actin mRNA levels (Table 1).

Nephrin mRNA levels were measured by double-stranded DNA (dsDNA) dye based RT-qPCR with Maxima SYBR Green RT-qPCR Master Mix (Thermo Fisher Scientific Inc., Waltham, MA, USA), and the mRNA values were normalized to glyceraldehyde-3-phosphate dehydrogenase. Mean values are expressed as fold mRNA levels relative to the control using the formula $2^{-\Delta(\Delta Ct)}$ (Ct: cycle time, $\Delta CT = CT_{target} - CT_{normalizer}$ and $\Delta(\Delta CT) = \Delta CT_{stimulated} - \Delta CT_{control}$) [31].

Statistics

Two-way ANOVA with or without repeated measures were used for multiple comparisons. Post hoc analyses were done with Holm-Sidak's test. Logarithmic transformation of data was used if Bartlett's test indicated a significant inhomogeneity of variances. Variables of the two sub-groups within the BH/DXR and the CD/DXR groups were compared using unpaired t-test. Survival was analyzed according to the Kaplan-Meier method. The null hypothesis was rejected if $p < 0.05$. Data were expressed as means ±SEM if not specified otherwise. All statistical analysis was done with GraphPad Prism (version 6.01, GraphPad Software Inc, San Diego, CA, USA).

Results

Heart toxicity was absent 8 weeks after 5 mg/kg DXR

Histology of the heart did not show necrosis or other morphological alterations of cardiomyocytes. Massons's trichrom staining was devoid of collagen deposition, and connexin-43 immunostaining did not demonstrate any sign of cardiomyocyte damage. Thus, a single dose of 5 mg/kg DXR did not induce any detectable chronic heart damage (data not shown).

CD rats became moribund earlier than BH rats at both low and high doses of DXR

BH rats became moribund significantly later following the 5 mg/kg DXR dose, compared to CD rats (Figure 1/A). The first CD rat became moribund 75 days after DXR administration, and there were no survivors after day 90 from this strain. The first BH became moribund 86 days after DXR, and there were survivors even 159 days after DXR administration. The median survival after DXR was 85.5 days for the CD rats, while it was 100 days for the BH rats ($p<0.05$).

A higher dose of 10 mg/kg DXR led to a more severe outcome. The median survival of CD rats was 10 days compared to 15 days of the BH rats (Figure 1/B). DXR administration caused less severe kidney damage than subtotal nephrectomy (SNX) and salt + protein loading in our previous study [11] as demonstrated by longer survival.

DXR inhibited bodyweight gain more in CD than in BH rats

DXR-administration inhibited weight gain in BH and CD rats (Figure 2/A). BH rats had a slower growth rate than age matched CD rats. Bodyweight constantly increased in all control animals. Body weight gain was significantly inhibited in DXR-injected CD rats (CD/DXR) already starting at week 4 while CD/DXR rats started to lose weight by week 8. On the contrary, significant weight gain inhibition was observed in BH rats (BH/DXR) only at week 8.

Proteinuria was milder in BH than CD rats after DXR

Proteinuria was assessed as a marker of podocyte damage and progression of renal fibrosis. In the functional and morphological experiment (exp. 1) 5 mg/kg DXR induced progressive proteinuria commencing 2 weeks after DXR in CD rats (Figure 2/B). Proteinuria started later and progressed slower in BH than in CD rats, and proteinuria was significantly milder at each time-point in BH/DXR than in CD/DXR rats.

Urinary NGAL excretion - a known marker of tubular epithelial damage - increased in both DXR-injected groups after the fourth week. Similarly to proteinuria, NGAL excretion was significantly milder in the BH/DXR than in the CD/DXR group (Figure 2/C).

Renal histological damage and inflammation were more severe in CD than in BH rats 8 weeks after DXR

Both CD and BH rats injected with saline had normal kidneys with no or minimal glomerular and tubular abnormalities 8 weeks after the injection. DXR administration caused glomerular damage in all age-matched rats. However, BH/DXR rats had

milder glomerular and tubular damage compared to CD/DXR rats (Figure 3/A-F, Table 2). Glomerular and tubular damage were distributed unevenly in rats, similarly to human focal segmental glomerulosclerosis (FSGS) [18]. In parallel with milder proteinuria and urinary excretion of NGAL in BH rats, intact glomeruli (Score: 0) were significantly more common in DXR-injected BH than in CD rats (Table 2). However, mild (Score: 0.5-1.5) (CD: 50.7 vs. BH: 28.4 %) and severe (Score ≥ 2) (CD: 13.3 vs. BH: 3.3 %) glomerular damage was significantly more common in CD/DXR vs. BH/DXR rats. Probably as a consequence of different degrees of glomerular damage, tubulointerstitial damage was milder in BH than in CD rats (Table 2).

Eight weeks after DXR administration severe inflammatory infiltration by neutrophil granulocytes, lymphocytes and macrophages was evident in the kidney samples of DXR-injected CD rats. In parallel with less proteinuria and morphological damage, inflammation was significantly milder in BH/DXR rats than in CD rats (Figure 3/G-I).

Milder fibrosis was associated with less oxidative stress and inflammation

Fibrosis was strikingly more intense in CD/DXR than in BH/DXR rats as demonstrated by Sirius red staining (Figure 3/J,K). Fibronectin immunostaining was detected only in 5.2±0.6 % of the scanned areas in the saline-injected control groups, but increased significantly in the DXR-injected CD group. Significantly less fibronectin staining was detected in BH/DXR than in CD/DXR rats (Figure 3/L,M).

TGF-β1 and CTGF mRNA levels in the kidney cortex were not significantly different in the control groups compared to DXR-injected BH rats, but were significantly

elevated in the CD/DXR group (Figure 4/A,B). COL1A1 mRNA levels were elevated in DXR-injected rats, but the elevation was significantly higher in the CD/DXR group than in the BH/DXR group (Figure 4/C).

Nephrin is an important component of the podocyte foot processes forming the slit diaphragm. It plays an important role in the maintenance of the structural integrity and the functional soundness of the slit diaphragm [32]. Nephrin mRNA levels decreased in the kidney cortex of the CD/DXR group, but it was not reduced in the BH/DXR group (Figure 4/D) supporting further a milder glomerular damage in BH/DXR rats.

The mRNA levels of pro-inflammatory monocyte chemotactic protein 1 (MCP-1) (Figure 4/E) and pro-oxidant markers: $p91^{phox}$ and $p47^{phox}$ (Figure 4/F,G) increased in both DXR-injected groups; however the elevation was milder in the BH/DXR group.

4-hydroxy-2-nonenal and nitrotyrosine

In the background of more severe kidney function deterioration demonstrated by proteinuria and fibrosis markers, severe lipid peroxidation and nitrative stress were detected in the kidneys of DXR-injected CD rats, while very mild changes were seen in the HNE or NT stained paraffin sections from the BH/DXR rats. Less staining was corroborated by Western blot demonstrating significantly more HNE and NT in CD than in BH rats 8 weeks after DXR administration (Figure 5).

Tubulointerstitial fibrosis and inflammation were milder in DXR-treated BH vs. CD rats despite similar proteinuria

Urinary protein excretion and renal nephrin mRNA levels were similar in the two subgroups of CD and BH rats (BH/DXRp, CD/DXRp) with similar proteinuria (Table 3). Markers of fibrosis such as sirius red staining and relative renal expression of TGF-β1, CTGF, COL1A1 were significantly lower in BH/DXRp vs. CD/DXRp rats. Paralleling less fibrosis, tubular damage detected by urinary NGAL excretion, markers of oxidative damage such as $p47^{phox}$ and $p91^{phox}$ expression and inflammation (MCP-1 expression) were significantly lower in BH/DXRp than CD/DXRp rats (Table 3).

Discussion

Renal fibrosis is an intractable medical condition with high mortality and low quality of life. We present here an animal model useful to investigate the pathomechanisms of hereditary susceptibility or resistance to renal fibrosis in various kidney injury models [10,33,34]. We demonstrated recently that BH rats were resistant to renal fibrosis with better preserved renal function and glomerular structure in a clinically relevant model of subtotal nephrectomy combined with salt and protein loading [11]. In the present study we demonstrate that less oxidative/nitrative stress and inflammation was associated with slower progression of fibrosis in the resistant strain. Taken together with our previous report demonstrating similar resistance of BH vs. CD rats in the subtotal nephrectomy model, our present findings underline the pathophysiological relevance of inflammation and oxidative/nitrative stress pathways in fibrosis progression.

DXR nephropathy in rodents is a widely used experimental model of human FSGS [12,35]. Direct exposure of the kidneys to DXR is a requirement for the development of podocyte injury in rats, as clipping the renal artery during DXR injection prevents nephropathy [35]. A single intravenous injection with 4-7,5 mg/kg DXR led to well predictable deterioration of glomerular structure, proteinuria, tubular and interstitial inflammation culminating in renal fibrosis in fibrosis-sensitive Sprague Dawley or Wistar rats [36]. Glomerular structural changes develop in a well predictable manner: altered mRNA levels of nephrin, podocyn and NEPH1, and swelling of the foot-processes are present at day 7 [37]. Podocyte swelling with cytoplasmic vesicles appear at day 14, and finally widespread podocyte foot process fusion at day 28 [38]. As a marker of glomerular filtration barrier damage, proteinuria develops [39].

Repeated low dose DXR has been widely used to induce toxic cardiomyopathy. In our model cardiac toxicity was absent after a single DXR injection, as demonstrated by histology or the sensitive cardiomyopathy marker Cx-43.

BH rats have a slower growth rate than age matched CD rats under healthy circumstances. The body weight curve in control animals of our study were similar to the previous findings [40,41].

In our study, sensitive CD rats developed significant and progressive proteinuria starting two weeks after 5 mg/kg DXR similarly to that shown in previous publications [37-42]. Nephrin plays an important role in maintaining the structural integrity and the functional soundness of the slit diaphragm [32]. In the background of the proteinuria significant nephrin loss was demonstrated in CD rats. The severity of proteinuria was milder and progression was slower in BH rats. Thus, as BH rats had similar nephrin mRNA levels to the strain-identical controls, nephrin might play a central role in the progression of DXR-induced fibrosis. Proteinuria-associated interstitial fibrosis and tubular atrophy (IFTA) has been recognized previously [43]. Podocyte dysfunction and consequent proteinuria has been recently reinforced as a major determinant of tubular injury, inflammation and apoptosis leading to progressive IFTA [44]. According to our present study and previous literature [45] IFTA developed as part of DXR nephropathy. Urinary NGAL excretion is a sensitive marker of tubular damage not only during acute kidney injury [46,47,] but also during IFTA [48]. In our study, significantly less proteinuria was accompanied by reduced tubular damage and less urinary NGAL excretion after DXR in the BH than in the CD strain. Similarly, less renal damage and less proteinuria was accompanied by better maintained body weight and significantly prolonged survival in BH rats. These data support that IFTA is secondary to proteinuria in the DXR model. The single administration of DXR and

consequent albuminuria led to tubulointerstitial inflammation and fibrosis demonstrated by PAS, Sirius red and fibronectin and collagen synthesis and the presence of the pro-fibrotic transforming growth factor (TGF-β1) [49,50,] and its downstream mediator connective tissue growth factor (CTGF) [51]. Significant reduction of these fibrotic pathways in the resistant BH strain underlines the relevance of the TGF-β1-CTGF cascade-mediated matrix deposition in the development of DXR-induced renal fibrosis (Figure 6).

Oxidative and nitrative stress has been proposed as the mechanism by which DXR induces glomerular toxicity in rats. Redox cycling of the quinone functional group of DXR was proposed as the key factor in DXR nephrotoxicity [52]. Reactive oxygen species (ROS) may initiate a degenerative cascade by the oxidation of cellular thiols and lipid membrane structures [53]. DXR has been suggested to upregulate NADPH-oxidase (NOX), an important source of ROS in the kidney [54]. However, the role of oxidative mechanisms in DXR toxicity has been questioned as well [55]. In our study, signs of lipid peroxidation and nitrative stress were milder in the BH rats, compared to the CD rats suggesting that less oxidative and nitrative stress may be responsible, at least in part, for the resistance of BH rats against renal fibrosis. This observation supports the role of oxidative and nitrative mechanisms in DXR toxicity.

Our results obtained in the subgroups of DXR-treated CD and BH rats with similar urinary protein excretion support our view that BH rats are less susceptible to tubulointerstital fibrosis induced by proteinuria. Renal nephrin mRNA expression was similar in the two subgroups, suggesting that the degree of podocyte injury and slit diaphragm leakiness is a primary determinant of proteinuria independent of the genetic background. However, despite similar proteinuria, most markers of renal fibrosis, oxidative stress and inflammation were significantly lower in BH rats. These

results support the role of inflammation in proteinuria-induced tubulointerstitial fibrosis.

Resistance mechanisms against DXR nephropathy were studied previously in rat [56] and mouse [57] strains. In spontaneously hypertensive (SHR) rats, cardio- and nephrotoxicity of DXR was more severe than in congenic Wistar-Kyoto (WKY) and in SHR-heart failure rats after subsequent administration of 2 mg/kg DXR on 8 consecutive days. Twelve weeks after the last dose of DXR renal lesions were similar to those in our study with podocyte adhesion leading to glomerulosclerosis and mononuclear infiltration, tubular atrophy and fibrotic matrix expansion in the tubulointerstitium [56]. Severity of these histological changes correlated with strain sensitivity. Similarly to our study, strain differences were partially explained by a difference in the severity of inflammation and arachidonic acid metabolism.

Sensitivity to DXR nephropathy was investigated previously in fibrosis-resistant C57BL/6 and -sensitive BALB/c mice [10]. The difference in susceptibility was attributed to a mutation in the PRKDC gene encoding the **c**atalytic subunit of a DNA activated protein kinase (DNA-PK), a double stranded break repair protein [10,58]. This mutation is also responsible for the severe combined immunodeficiency (SCID) phenotype in mice and rats [59]. DNA-PK expression and activity was also profoundly lower in BALB/c than C57BL/6 mice in a radiation induced apoptosis model [60]. Thus, DNA-PK seems to be crucial in toxic injury models. As inflammation and related oxidative stress also induces DNA damage, the PRKDC gene may play an important role also in our model.

Fibrosis is mediated by myofibroblasts activated by TGF-β1, MCP-1, etc. [61]. In our study, decreased MCP-1 mRNA levels were found in resistant BH rats, which is one of the key chemokines for the migration and infiltration of macrophages to sites of

inflammation [62]. The mRNA levels of p91^{phox}, also known as NADPH oxidase 2 (NOX2) were also lower in BH rats. NOX2 plays an important role in ROS production of phagocytes and T cells. Furthermore, the mRNA level of p47^{phox}, which plays a role in the activation of the NOX2/p22^{phox} complex in the membrane of phagocytes [63], was also milder in BH rats. These findings suggest that less inflammation, accompanied by milder ROS production of the neutrophil cells and macrophages may play a role in the resistance of BH rats against DXR nephropathy.

Conclusions:

In conclusion, resistance of BH rats against renal fibrosis highlighted the role of inflammation-induced oxidative/nitrative stress in chronic podocyte injury leading to glomerulosclerosis and consequent proteinuria in DXR nephropathy. Tubulointerstitial fibrosis is most likely secondary to proteinuria in this model.

Acknowledgements

Support was provided to P. Hamar from the Hungarian Research Fund: OTKA-ANN(FWF) 110810 and OTKA-SNN 114619, and to P. Pacher from the Intramural Research Program of NIAAA/NIH. P Hamar acknowledges support from the Bolyai Research Scholarship of the Hungarian Academy of Sciences and the Merit Prize of the Semmelweis University.

We wish to thank Róbert Glávits, DVM, PhD, DSc for his help in the histological assessment of the kidney samples.

References

1. Comas J, Arcos E, Castell C, Cases A, Martinez-Castelao A, et al. (2013) Evolution of the incidence of chronic kidney disease Stage 5 requiring renal replacement therapy in the diabetic population of Catalonia. Nephrol Dial Transplant 28: 1191-1198.
2. (2014) National Chronic Kidney Disease Fact Sheet. Available: http://wwwcdcgov/diabetes/pubs/factsheets/kidneyhtm Accessed 3 August 2014.
3. Boor P, Floege J (2011) Chronic kidney disease growth factors in renal fibrosis. Clin Exp Pharmacol Physiol 38: 441-450.
4. Hostetter TH, Olson JL, Rennke HG, Venkatachalam MA, Brenner BM (2001) Hyperfiltration in remnant nephrons: a potentially adverse response to renal ablation. J Am Soc Nephrol 12: 1315-1325.
5. Cameron JS (1996) The enigma of focal segmental glomerulosclerosis. Kidney Int Suppl 57: S119-131.
6. Fitzgibbon WR, Greene EL, Grewal JS, Hutchison FN, Self SE, et al. (1999) Resistance to remnant nephropathy in the Wistar-Furth rat. J Am Soc Nephrol 10: 814-821.
7. Fleck C, Appenroth D, Jonas P, Koch M, Kundt G, et al. (2006) Suitability of 5/6 nephrectomy (5/6NX) for the induction of interstitial renal fibrosis in rats--influence of sex, strain, and surgical procedure. Exp Toxicol Pathol 57: 195-205.
8. Rostand SG, Kirk KA, Rutsky EA, Pate BA (1982) Racial differences in the incidence of treatment for end-stage renal disease. N Engl J Med 306: 1276-1279.
9. Kaplan JM, Kim SH, North KN, Rennke H, Correia LA, et al. (2000) Mutations in ACTN4, encoding alpha-actinin-4, cause familial focal segmental glomerulosclerosis. Nat Genet 24: 251-256.
10. Papeta N, Chan KT, Prakash S, Martino J, Kiryluk K, et al. (2009) Susceptibility loci for murine HIV-associated nephropathy encode trans-regulators of podocyte gene expression. J Clin Invest 119: 1178-1188.
11. Kokeny G, Nemeth Z, Godo M, Hamar P (2010) The Rowett rat strain is resistant to renal fibrosis. Nephrol Dial Transplant 25: 1458-1462.
12. Lee VW, Harris DC (2011) Adriamycin nephropathy: a model of focal segmental glomerulosclerosis. Nephrology (Carlton) 16: 30-38.
13. Zhu C, Xuan X, Che R, Ding G, Zhao M, et al. (2014) Dysfunction of the PGC-1alpha-mitochondria axis confers adriamycin-induced podocyte injury. Am J Physiol Renal Physiol 306: F1410-1417.
14. Tapia E, Soto V, Ortiz-Vega KM, Zarco-Marquez G, Molina-Jijon E, et al. (2012) Curcumin induces Nrf2 nuclear translocation and prevents glomerular hypertension, hyperfiltration, oxidant stress, and the decrease in antioxidant enzymes in 5/6 nephrectomized rats. Oxid Med Cell Longev 2012: 269039.
15. Toba H, Nakashima K, Oshima Y, Kojima Y, Tojo C, et al. (2010) Erythropoietin prevents vascular inflammation and oxidative stress in subtotal nephrectomized rat aorta beyond haematopoiesis. Clin Exp Pharmacol Physiol 37: 1139-1146.
16. Rashid S, Ali N, Nafees S, Ahmad ST, Arjumand W, et al. (2013) Alleviation of doxorubicin-induced nephrotoxicity and hepatotoxicity by chrysin in Wistar rats. Toxicol Mech Methods 23: 337-345.
17. Park EJ, Kwon HK, Choi YM, Shin HJ, Choi S (2012) Doxorubicin induces cytotoxicity through upregulation of pERK-dependent ATF3. PLoS One 7: e44990.
18. Ma H, Wu Y, Zhang W, Dai Y, Li F, et al. (2013) The effect of mesenchymal stromal cells on doxorubicin-induced nephropathy in rats. Cytotherapy 15: 703-711.
19. Polhill T, Zhang GY, Hu M, Sawyer A, Zhou JJ, et al. (2012) IL-2/IL-2Ab complexes induce regulatory T cell expansion and protect against proteinuric CKD. J Am Soc Nephrol 23: 1303-1308.
20. Takimoto CC, E. (2008) "Principles of Oncologic Pharmacotherapy". In: Pazdur R, Camphausen KA, Wagman LD, Hoskins WJ, editors. Cancer Management: A Multidisciplinary Approach. 11. ed ed: Cmp United Business Media.
21. Fujimura T, Yamagishi S, Ueda S, Fukami K, Shibata R, et al. (2009) Administration of pigment epithelium-derived factor (PEDF) reduces proteinuria by suppressing decreased nephrin and increased VEGF expression in the glomeruli of adriamycin-injected rats. Nephrol Dial Transplant 24: 1397-1406.

22. Ramadan R, Faour D, Awad H, Khateeb E, Cohen R, et al. (2012) Early treatment with everolimus exerts nephroprotective effect in rats with adriamycin-induced nephrotic syndrome. Nephrol Dial Transplant 27: 2231-2241.
23. Deman A, Ceyssens B, Pauwels M, Zhang J, Houte KV, et al. (2001) Altered antioxidant defence in a mouse adriamycin model of glomerulosclerosis. Nephrol Dial Transplant 16: 147-150.
24. Wu H, Wang Y, Tay YC, Zheng G, Zhang C, et al. (2005) DNA vaccination with naked DNA encoding MCP-1 and RANTES protects against renal injury in adriamycin nephropathy. Kidney Int 67: 2178-2186.
25. Mahajan D, Wang Y, Qin X, Wang Y, Zheng G, et al. (2006) CD4+CD25+ regulatory T cells protect against injury in an innate murine model of chronic kidney disease. J Am Soc Nephrol 17: 2731-2741.
26. Liu S, Jia Z, Zhou L, Liu Y, Ling H, et al. (2013) Nitro-oleic acid protects against adriamycin-induced nephropathy in mice. Am J Physiol Renal Physiol 305: F1533-1541.
27. Hamar P, Liptak P, Heemann U, Ivanyi B (2005) Ultrastructural analysis of the Fisher to Lewis rat model of chronic allograft nephropathy. Transpl Int 18: 863-870.
28. el Nahas AM, Zoob SN, Evans DJ, Rees AJ (1987) Chronic renal failure after nephrotoxic nephritis in rats: contributions to progression. Kidney Int 32: 173-180.
29. Hamar P, Kokeny G, Liptak P, Krtil J, Adamczak M, et al. (2007) The combination of ACE inhibition plus sympathetic denervation is superior to ACE inhibitor monotherapy in the rat renal ablation model. Nephron Exp Nephrol 105: e124-136.
30. Fang L, Radovits T, Szabo G, Mozes MM, Rosivall L, et al. (2013) Selective phosphodiesterase-5 (PDE-5) inhibitor vardenafil ameliorates renal damage in type 1 diabetic rats by restoring cyclic 3',5' guanosine monophosphate (cGMP) level in podocytes. Nephrol Dial Transplant 28: 1751-1761.
31. Livak KJ, Schmittgen TD (2001) Analysis of relative gene expression data using real-time quantitative PCR and the 2(-Delta Delta C(T)) Method. Methods 25: 402-408.
32. Machado JR, Rocha LP, Neves PD, Cobo Ede C, Silva MV, et al. (2012) An overview of molecular mechanism of nephrotic syndrome. Int J Nephrol 2012: 937623.
33. Chua S, Jr., Li Y, Liu SM, Liu R, Chan KT, et al. (2010) A susceptibility gene for kidney disease in an obese mouse model of type II diabetes maps to chromosome 8. Kidney Int 78: 453-462.
34. Zheng Z, Pavlidis P, Chua S, D'Agati VD, Gharavi AG (2006) An ancestral haplotype defines susceptibility to doxorubicin nephropathy in the laboratory mouse. J Am Soc Nephrol 17: 1796-1800.
35. de Mik SM, Hoogduijn MJ, de Bruin RW, Dor FJ (2013) Pathophysiology and treatment of focal segmental glomerulosclerosis: the role of animal models. BMC Nephrol 14: 74.
36. Bertani T, Rocchi G, Sacchi G, Mecca G, Remuzzi G (1986) Adriamycin-induced glomerulosclerosis in the rat. Am J Kidney Dis 7: 12-19.
37. Otaki Y, Miyauchi N, Higa M, Takada A, Kuroda T, et al. (2008) Dissociation of NEPH1 from nephrin is involved in development of a rat model of focal segmental glomerulosclerosis. Am J Physiol Renal Physiol 295: F1376-1387.
38. Fan Q, Xing Y, Ding J, Guan N (2009) Reduction in VEGF protein and phosphorylated nephrin associated with proteinuria in adriamycin nephropathy rats. Nephron Exp Nephrol 111: e92-e102.
39. Jeansson M, Bjorck K, Tenstad O, Haraldsson B (2009) Adriamycin alters glomerular endothelium to induce proteinuria. J Am Soc Nephrol 20: 114-122.
40. (2014) Charles River Laboratories: RNU rat. Available: http://wwwcrivercom/products-services/basic-research/find-a-model/rnu-rat Accessed: 30 November 2014.
41. Pettersen JC, Morrissey RL, Saunders DR, Pavkov KL, Luempert LG, 3rd, et al. (1996) A 2-year comparison study of Crl:CD BR and Hsd:Sprague-Dawley SD rats. Fundam Appl Toxicol 33: 196-211.
42. Zou MS, Yu J, Nie GM, He WS, Luo LM, et al. (2010) 1, 25-dihydroxyvitamin D3 decreases adriamycin-induced podocyte apoptosis and loss. Int J Med Sci 7: 290-299.
43. Gross ML, Hanke W, Koch A, Ziebart H, Amann K, et al. (2002) Intraperitoneal protein injection in the axolotl: the amphibian kidney as a novel model to study tubulointerstitial activation. Kidney Int 62: 51-59.
44. Zoja C, Abbate M, Remuzzi G (2014) Progression of renal injury toward interstitial inflammation and glomerular sclerosis is dependent on abnormal protein filtration. Nephrol Dial Transplant.

45. Cianciolo R, Yoon L, Krull D, Stokes A, Rodriguez A, et al. (2013) Gene expression analysis and urinary biomarker assays reveal activation of tubulointerstitial injury pathways in a rodent model of chronic proteinuria (Doxorubicin nephropathy). Nephron Exp Nephrol 124: 1-10.
46. Mishra J, Ma Q, Prada A, Mitsnefes M, Zahedi K, et al. (2003) Identification of neutrophil gelatinase-associated lipocalin as a novel early urinary biomarker for ischemic renal injury. J Am Soc Nephrol 14: 2534-2543.
47. Mishra J, Dent C, Tarabishi R, Mitsnefes MM, Ma Q, et al. (2005) Neutrophil gelatinase-associated lipocalin (NGAL) as a biomarker for acute renal injury after cardiac surgery. Lancet 365: 1231-1238.
48. Entin-Meer M, Ben-Shoshan J, Maysel-Auslender S, Levy R, Goryainov P, et al. (2012) Accelerated renal fibrosis in cardiorenal syndrome is associated with long-term increase in urine neutrophil gelatinase-associated lipocalin levels. Am J Nephrol 36: 190-200.
49. Lan HY (2011) Diverse roles of TGF-beta/Smads in renal fibrosis and inflammation. Int J Biol Sci 7: 1056-1067.
50. Yanagita M (2012) Inhibitors/antagonists of TGF-beta system in kidney fibrosis. Nephrol Dial Transplant 27: 3686-3691.
51. Ruster C, Wolf G (2011) Angiotensin II as a morphogenic cytokine stimulating renal fibrogenesis. J Am Soc Nephrol 22: 1189-1199.
52. Fukuda F, Kitada M, Horie T, Awazu S (1992) Evaluation of adriamycin-induced lipid peroxidation. Biochem Pharmacol 44: 755-760.
53. Qin XJ, He W, Hai CX, Liang X, Liu R (2008) Protection of multiple antioxidants Chinese herbal medicine on the oxidative stress induced by adriamycin chemotherapy. J Appl Toxicol 28: 271-282.
54. Guo J, Ananthakrishnan R, Qu W, Lu Y, Reiniger N, et al. (2008) RAGE mediates podocyte injury in adriamycin-induced glomerulosclerosis. J Am Soc Nephrol 19: 961-972.
55. Morgan WA, Kaler B, Bach PH (1998) The role of reactive oxygen species in adriamycin and menadione-induced glomerular toxicity. Toxicol Lett 94: 209-215.
56. Sharkey LC, Radin MJ, Heller L, Rogers LK, Tobias A, et al. (2013) Differential cardiotoxicity in response to chronic doxorubicin treatment in male spontaneous hypertension-heart failure (SHHF), spontaneously hypertensive (SHR), and Wistar Kyoto (WKY) rats. Toxicol Appl Pharmacol 273: 47-57.
57. Zheng Z, Schmidt-Ott KM, Chua S, Foster KA, Frankel RZ, et al. (2005) A Mendelian locus on chromosome 16 determines susceptibility to doxorubicin nephropathy in the mouse. Proc Natl Acad Sci U S A 102: 2502-2507.
58. Papeta N, Zheng Z, Schon EA, Brosel S, Altintas MM, et al. (2010) Prkdc participates in mitochondrial genome maintenance and prevents Adriamycin-induced nephropathy in mice. J Clin Invest 120: 4055-4064.
59. Mashimo T, Takizawa A, Kobayashi J, Kunihiro Y, Yoshimi K, et al. (2012) Generation and characterization of severe combined immunodeficiency rats. Cell Rep 2: 685-694.
60. Mori N, Matsumoto Y, Okumoto M, Suzuki N, Yamate J (2001) Variations in Prkdc encoding the catalytic subunit of DNA-dependent protein kinase (DNA-PKcs) and susceptibility to radiation-induced apoptosis and lymphomagenesis. Oncogene 20: 3609-3619.
61. Wynn TA (2008) Cellular and molecular mechanisms of fibrosis. J Pathol 214: 199-210.
62. Zhang Y, Bao S, Kuang Z, Ma Y, Hu Y, et al. (2014) Urotensin II promotes monocyte chemoattractant protein-1 expression in aortic adventitial fibroblasts of rat. Chin Med J (Engl) 127: 1907-1912.
63. Lee K, Won HY, Bae MA, Hong JH, Hwang ES (2011) Spontaneous and aging-dependent development of arthritis in NADPH oxidase 2 deficiency through altered differentiation of CD11b+ and Th/Treg cells. Proc Natl Acad Sci U S A 108: 9548-9553.

Figure legends

Figure 1: Survival (long term: **A,** short term: **B)**

CD: CD rats, BH: BH rats. DXR: Doxorubicin injected rats (5 mg/kg).

Figure 2: Body weight changes (A) proteinuria (B) and urinary NGAL excretion (C)

CD: CD rats, BH: BH rats. c: saline-injected, DXR: Doxorubicin-injected rats (5 mg/kg).

*: $p<0.05$ vs. strain-identical, negative control group, †: $p<0.05$ vs. CD/DXR, positive control group.

Figure 3: Renal histopathology

Top row (periodic acid–Schiff (PAS) staining) (**A-C**): Glomerular damage in the affected areas.

Middle row PAS staining) (**D-F**): Tubular damage in the affected areas.

Lower row (hematoxylin-eosin (HE) staining) (**G-I**): Tubulointerstitial inflammatory infiltration.

Saline-injected control rats (**A,D,G**); CD-DXR: doxorubicin-injected (5 mg/kg) CD rats (**B,E,H**); BH-DXR: doxorubicin-injected BH rats (**C,F,I**)

J: Sirius red staining (100x)

L: Fibronectin immunohistochemistry (400x)

K, M: computerized quantification of the immunostained areas

CD: CD rats, BH: BH rats. c: saline-injected, DXR: Doxorubicin-injected rats (5 mg/kg).

*: $p<0.05$ vs. strain-identical, control group, †: $p<0.05$ vs. CD/DXR, control group.

Figure 4: Renal cortical mRNA levels of fibrosis related, inflammatory and oxidative markers

(**A:** TGF-β1, **B:** CTGF, **C:** COL1A1, **D:** nephrin, **E:** MCP-1 **F:** $p47^{phox}$, **G**: $p91^{phox}$

CD: CD rats, BH: BH rats. c: saline-injected, DXR: Doxorubicin-injected rats (5 mg/kg).

TGF-β1: transforming growth factor β1; CTGF: connective tissue growth factor; COL1A1: collagen type I alpha 1; MCP-1: monocyte chemotactic protein 1; $p47^{phox}$: neutrophil cytosolic factor 1; $p91^{phox}$: cytochrome b-245, beta polypeptide;

*: $p<0.05$ vs. strain-identical control group, †: $p<0.05$ vs. CD/DXR.

Figure 5: Oxidative/nitrative stress markers.

A: 4-hydroxy-2-nonenal (HNE) immunhistology (400x) and **B**: quantification by Western blot.

C: Nitrotyrosine (NT) immunohistology (400x) and **D:** quantification by Western blot.

CD: CD rats, BH: BH rats. c: saline-injected, DXR: Doxorubicin-injected rats (5 mg/kg).

Figure 6: Suggested mechanisms of doxorubicin induced nephropathy.

A single administration of doxorubicin induced podocyte damage demonstrated by loss of nephrin and leading to proteinuria. Proteinuria damages tubules as demonstrated by increased urinary NGAL excretion. Tubular damage leads to interstitial inflammation and fibrosis with collagen and fibronectin deposition. Inflammation is accompanied by oxidative/nitrative damage triggering further immune activation. Reverse arrows symbolize main elements of the vicious circle. Sustained injury activates the TGF-β1 and CTGF profibrotic axis. Sustained injury eventually leads to fibrotic end-stage kidney. NGAL: neutrophil gelatinase-associated lipocalin; TGF-β1: transforming growth factor β1; CTGF: connective tissue growth factor

Tables

Table 1: Qiagen primer reference numbers

Gene	Reference sequence	Qiagen primer reference number
p91^{phox} (NOX2)	NM_023965.1	QT00195300
p47^{phox} (Ncf1)	NM_053734	QT00189728
MCP-1 (Ccl2)	NM_031530.1	QT00183253
TGF-β1	NM_021578.2	QT00187796
CTGF	NM_022266.2	QT00182021
COL1A1	NM_053304.1	QT02285619

Table 2: Renal morphology:

Groups	Undamaged glomeruli (%)	Glomerulosclerosis score	Tubular score	Inflammation score
CD/DXR	36.3±13.4	0.79±0.22	2.01±0.64	1.61±0.32
BH/DXR	68.3±8.4	0.32±0.11	0.86±0.44	1.06±0.20
Control	93.3±4.4	0.06±0.04	0.00±0.00	0.18±0.06

P value (CD/DXR vs. BH/DXR)	<0.001	<0.001	<0.001	<0.01

CD: CD rats, BH: BH rats. Control: saline-injected, DXR: Doxorubicin-injected rats (5 mg/kg).

Mean±SD, n=10/group.

Table 3: Comparison of doxorubicin-injected (DXR) Rowett, black hooded (BH) and Charles Dawley (CD) rats with similar proteinuria (BH/DXRp and CD/DXRp subgroups):

	CD/DXRp (n=4)	BH/DXRp (n=5)	P value
U Protein, week 8 (mg/24h)	396.5±82.2	362.5±30.3	0.42
Nephrin	0.68±0.16	0.87±0.19	0.19
U NGAL, week 8 (mg/24h)	10.1±2.0	5.2±1.6	**<0.01**
Sirius red (%)	18.0±1.6	11.8±1.0	**<0.01**
Fibronectin (%)	7.91±2.45	5.55±1.19	0.16
TGF-β1	6.00±2.36	2.13±1.23	**<0.05**
CTGF	3.71±2.10	0.54±0.11	**<0.05**
COL1A1	23.09±6.14	5.79±2.41	**<0.01**
$p47^{phox}$	4.69±1.51	1.95±0.36	**<0.05**
$p91^{phox}$	10.69±2.47	1.94±0.78	**<0.01**
MCP-1	9.23 3.28	3.46±0.99	**<0.05**

Figure
Click here to download high resolution image

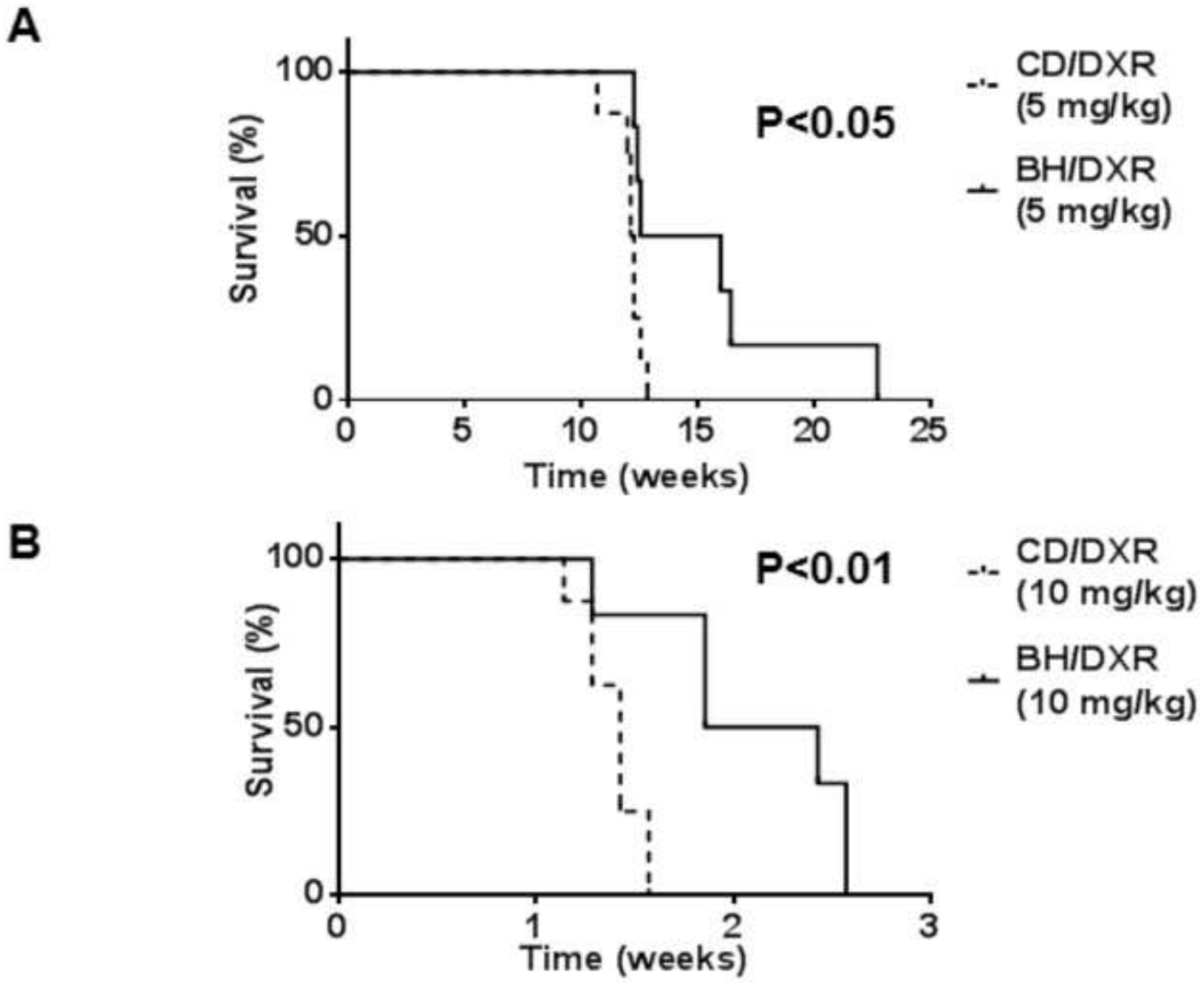

Figure
Click here to download high resolution image

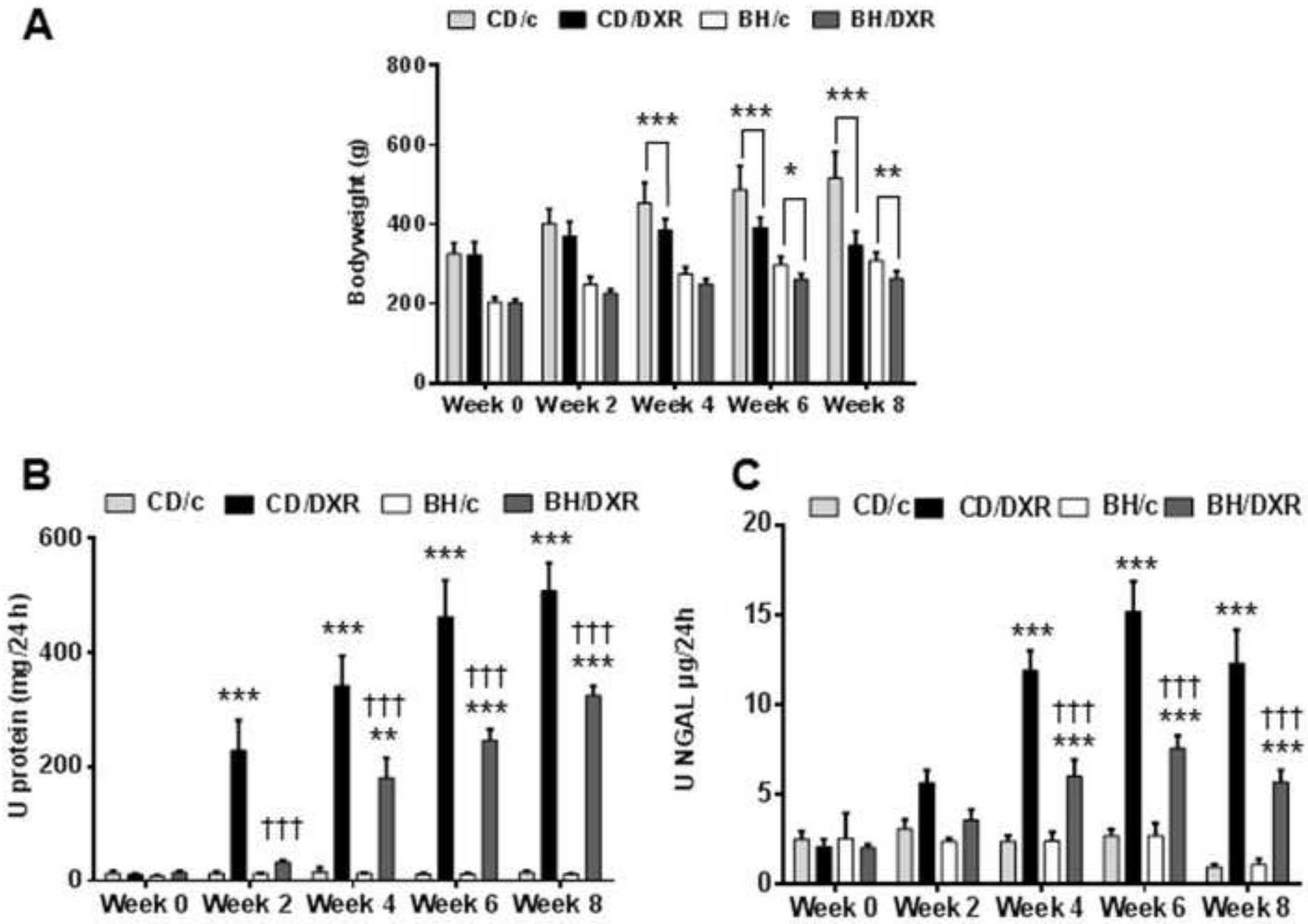

Figure
Click here to download high resolution image

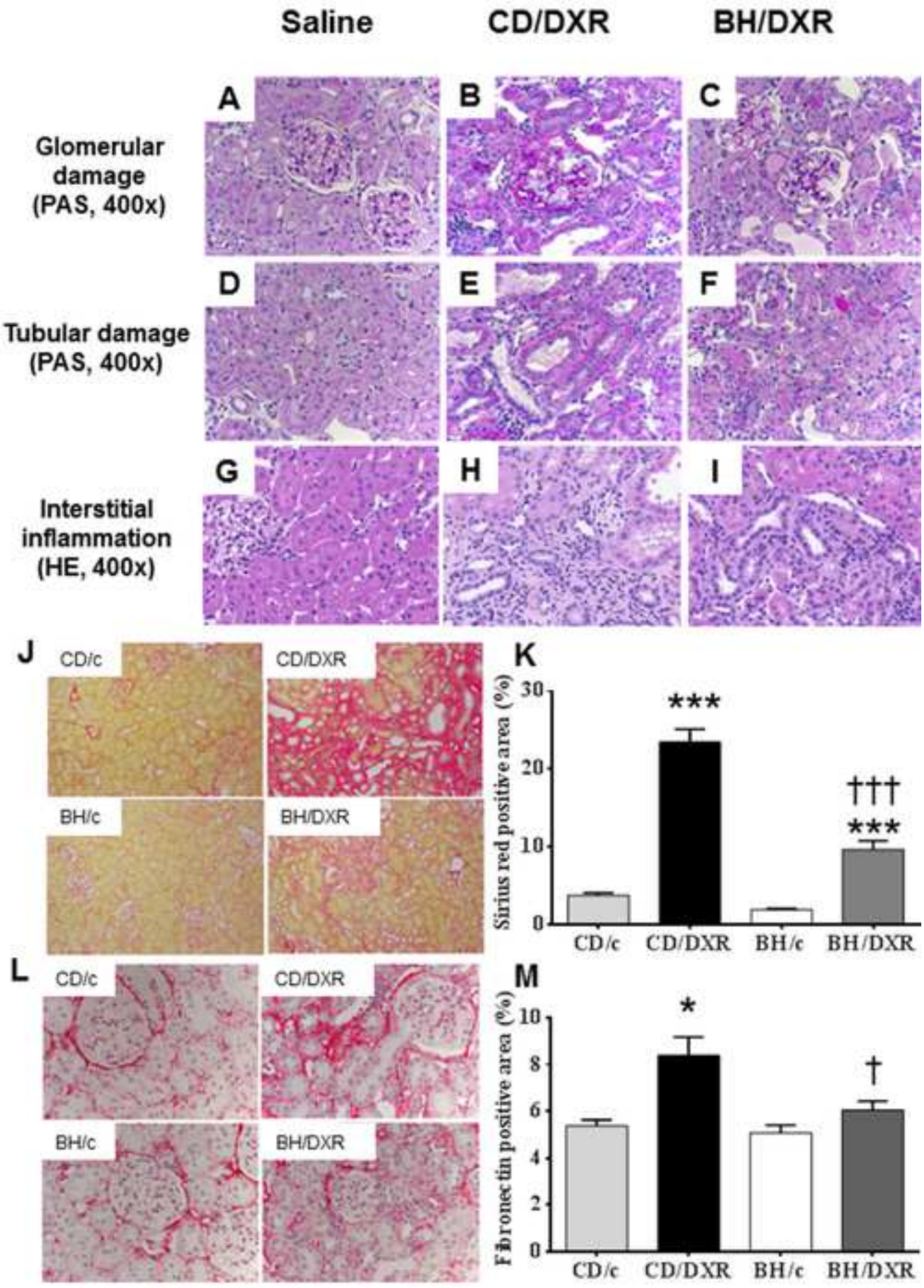

Figure
Click here to download high resolution image

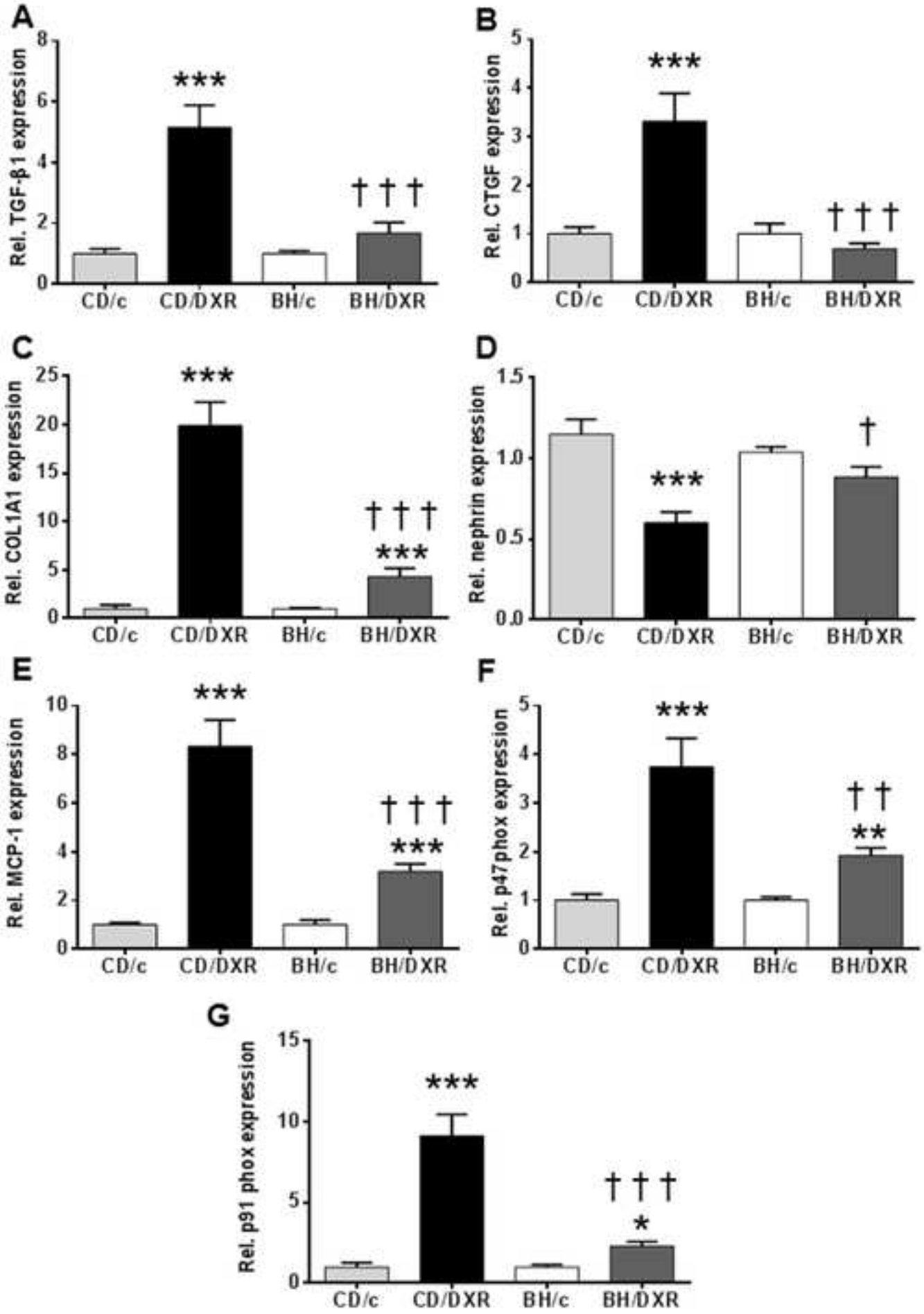

Figure
Click here to download high resolution image

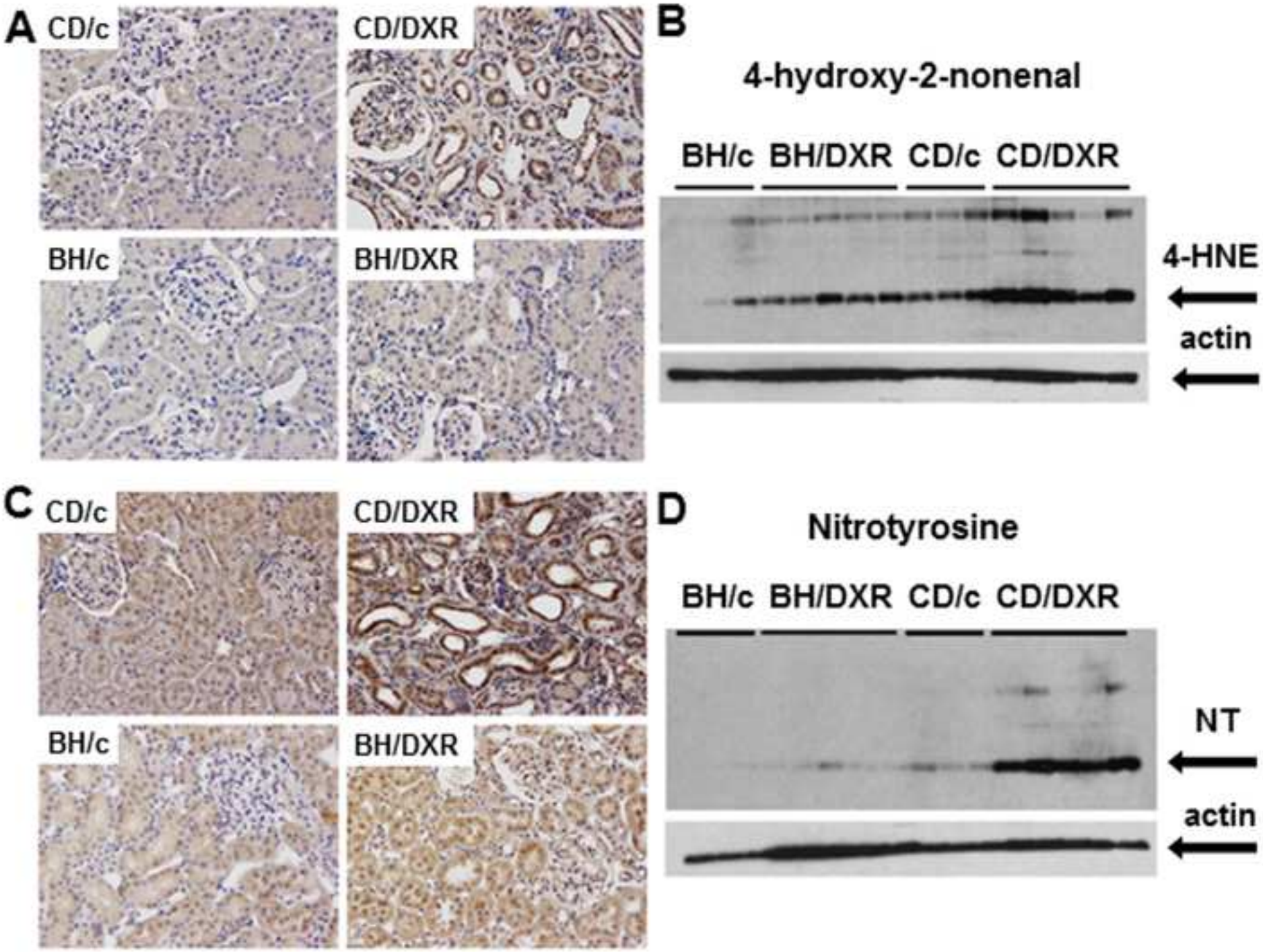

Figure
Click here to download high resolution image

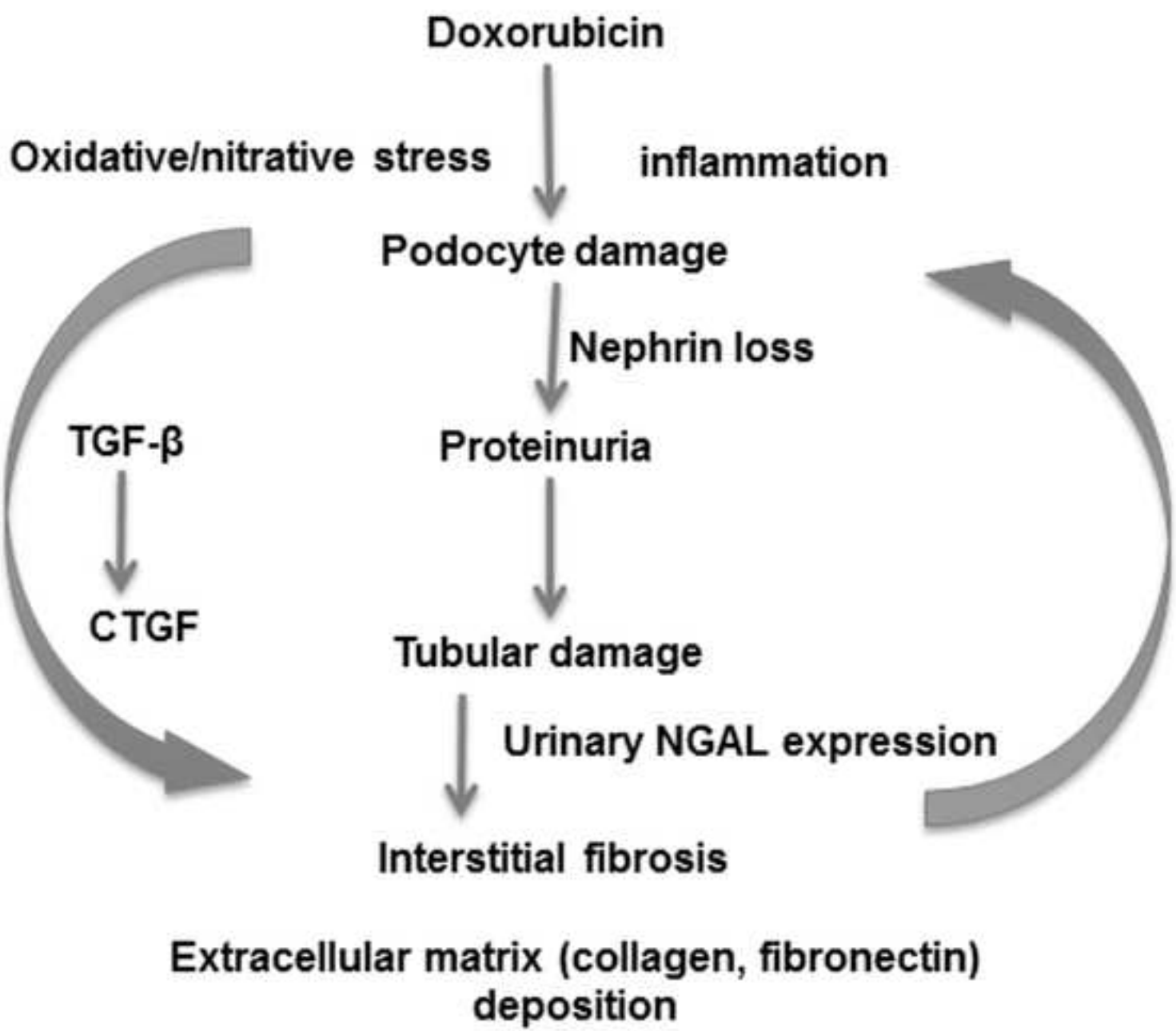

Oxidative/nitrative stress and inflammation drive progression of doxorubicin-induced renal fibrosis in rats as revealed by comparing a normal and a fibrosis-resistant rat strain

Authors: Csaba Imre Szalay[1], Katalin Erdelyi[2], Gábor Kökény[1], Enikő Lajtár[1], Mária Godó[1], Csaba Révész[1], Tamás Kaucsár[1], Norbert Kiss[1], Márta Sárközy[3], Tamás Csont[3], Tibor Krenács[4], Gábor Szénási[1], Pál Pacher[2¶], Péter Hamar[1¶*]

Affiliations:

[1] Semmelweis University, Institute of Pathophysiology, Budapest, Hungary

[2] National Institute of Health (NIH/NIAAA/DICBR), Laboratory of Physiological Studies, Section on Oxidative Stress and Tissue Injury, Bethesda, MD, USA

[3] University of Szeged, Faculty of Medicine, Department of Biochemistry, Szeged, Hungary

[4] 1st Semmelweis University, Department of Pathology and Experimental Cancer Research; MTA-SE Tumor Progression Research Group, Budapest, Hungary

* Corresponding author

E-mail: hamar.peter@med.semmelweis-univ.hu (PH)

¶: These authors contributed equally to this work.

Short title: Oxidative stress in renal fibrosis resistance

Key words: renal fibrosis, podocyte, oxidative stress, rat

List of abbreviations:

BH: black hooded, Rowett rats

BH/c or CD/c: control rats (injected with Saline)

BH/DXR or CD/DXR: doxorubicin-injected rats

CD: Charles Dawley rats

CKD: chronic kidney disease

COL1A1: collagen type I alpha 1

Ct: cycle time

CTGF: connective tissue growth factor

DXR: doxorubicin

FSGS: focal segmental glomerulosclerosis

~~GAPDH: glyceraldehyde-3-phosphate dehydrogenase~~

HNE: 4-hydroxy-2-nonenal

IFTA: Interstitial fibrosis and tubular atrophy

MCP-1: monocyte chemotactic protein 1

mRNA: messenger ribonucleic acid

NGAL: neutrophil gelatinase-associated lipocalin

NOX: nicotinamide adenine dinucleotide phosphate-oxidase

NT: nitrotyrosine

p47^{phox}: neutrophil cytosolic factor 1 (Ncf1~~)~~), neutrophil NOX-2 subunit

~~p91-phox~~p91^{phox}: NOX-2, cytochrome b-245 beta polypeptide, neutrophil NOX-2 subunit

Phox: Phagocyte oxidase

RT-qPCR: ~~-~~reverse transcription - quantitative polymerase chain reaction

ROS: reactive oxygen species

~~SHHF: SHR-heart failure~~

SHR: spontaneously hypertensive rats

TGF-β1: transforming growth factor β1

Abstract (word count: 294)

Chronic renal fibrosis is the final common pathway of end stage renal disease caused by glomerular or tubular pathologies. Genetic background has a strong influence on the progression of chronic renal fibrosis. We recently found that Rowett black hooded rats were resistant to renal fibrosis. We aimed to investigate the role of sustained inflammation and oxidative/nitrative stress in renal fibrosis progression using this new model. Our previous data suggested the involvement of podocytes, thus we investigated renal fibrosis initiated by doxorubicin-induced (5 mg/kg) podocyte damage. Doxorubicin induced progressive glomerular sclerosis followed by increasing proteinuria and reduced bodyweight gain in fibrosis-sensitive, Charles Dawley rats during an 8~~–~~-week long observation period. In comparison, the fibrosis-resistant, Rowett black hooded rats had longer survival, milder proteinuria and reduced tubular damage as assessed by neutrophil gelatinase-associated lipocalin (NGAL) excretion, reduced loss of the slit diaphragm protein, nephrin, less glomerulosclerosis, tubulointerstitial fibrosis and matrix deposition assessed by periodic acid–Schiff, Picro-Sirius-red staining and fibronectin ~~immune staining.~~immunostaining. Less fibrosis was associated with reduced profibrotic transforming growth factor-beta, (TGF-β1) connective tissue growth factor (CTGF), and collagen type I alpha 1 (COL-1a1) mRNA levels. Milder inflammation demonstrated by histology was confirmed by less monocyte chemotactic protein 1 (MCP-1) mRNA. As a consequence of less inflammation, less oxidative and nitrative stress was obvious by less neutrophil cytosolic factor 1 ($p47^{phox}$) and NADPH oxidase-2 (~~p91-phox~~$p91^{phox}$) mRNA. Reduced oxidative enzyme expression was accompanied by less lipid peroxidation as demonstrated by 4-hydroxynonenal (~~4-~~

HNE) and less protein nitrosylation demonstrated by nitrotyrosine (NT) immunohistochemistry and quantified by Western blot. Our results demonstrate that mediators of fibrosis, inflammation and oxidative/nitrative stress were suppressed in doxorubicin nephropathy in fibrosis-resistant Rowett black hooded rats underlying the importance of these pathomechanisms in the progression of renal fibrosis initiated by glomerular podocyte damage.

Introduction:

Chronic kidney disease (CKD) is a major healthcare problem with a prevalence of 7% in Europe [1], and over 10% in the US according to the Centers for Disease Control and Prevention [2]. The pathologic manifestation of CKD is renal fibrosis, which is the final common pathway of many kidney diseases, such as diabetic and hypertensive nephropathy, toxic, ischemic or autoimmune renal diseases [3,4].

The clinical presentation of CKD varies widely among patients with the same initial disease [5]. The severity of symptoms and the rate of CKD progression are influenced by age, gender [6,7] and numerous pieces of evidence support a role for genetic background in progression [8,9,10]. We have demonstrated previously that Rowett, black hooded (BH) rats were resistant to renal fibrosis induced by subtotal nephrectomy plus salt and protein loading [11]. Better understanding of such resistance can shed light on the pathomechanisms of fibrosis in general and renal fibrosis specifically.

The anthracycline derivative chemotherapeutic drug, Doxorubicin (Adriamycin, DXR) is widely used as a rodent model of proteinuric nephropathy leading to renal fibrosis [12]. Although it is generally accepted that an initial injury to podocytes induces proteinuria, the exact pathomechanism of the DXR-induced nephropathy is poorly understood [13]. The role of sustained inflammation and oxidative stress has been demonstrated in many experimental models of renal fibrosis, including the remnant kidney [11,14,15] and DXR nephropathy models [12,16,17,18,19]. The myocardial and renal side effects of DXR are mainly attributed to the generation of free oxygen radicals [20]. DXR exerts direct toxic damage to the glomerular structure leading to loss of nephrin [21] and consequent proteinuria [22]. Proteinuria per se, sustained

inflammation and accompanying oxidative damage are major mechanisms of progressive renal fibrosis [12]. It has been reported that the DXR-induced oxidative damage in cells of the renal cortex paralleled renal fibrosis progression [23]. DXR administration to rats led to severe tubulointerstitial inflammation with marked infiltration by T and B lymphocytes and macrophages. The intensity of inflammation correlated with the DXR-induced renal damage, and modifying pro-inflammatory pathways affected the severity of renal damage in this model [24,25,26].

We hypothesized that milder inflammation and milder accompanying oxidative/nitrative stress may be responsible for the previously published resistance of BH rats to renal fibrosis. To investigate the role of oxidative/nitrative stress and inflammation in the BH rats' protection from renal fibrosis, we compared CD and BH rats in ~~the~~ DXR~~-~~ nephropathy model.

Materials and Methods

Ethics Statement

Humane endpoints were used to minimize suffering in survival studies. Animals were observed and weighed every morning after potentially lethal interventions including DXR administration. If clinical signs of distress were recognized the animals were euthanized by cervical dislocation performed by a trained personnel. ~~Clinical signs of renal failure are described in the methods of survival study.~~ Uremic signs or body weight loss ~~exceeding~~> 40% of the initial body-weight was an indication for euthanasia. Clinical signs of uremia are described later. Sacrifice for organ removal was performed under ketamine + xylazin (CP-Ketamin 10%, ~~CP-Pharma, Burgdorf, Germany) + xylazin (~~CP-Xylazin 2%, CP-Pharma, Burgdorf, Germany) anesthesia.

All procedures were performed in accordance with guidelines set by the National Institutes of Health and the Hungarian law on animal care and protection. The experimental protocol was reviewed and approved by the “Institutional Ethical Committee for Animal Care and Use” of Semmelweis University (registration number: XIV-I-001/2104-4/2012).

Animals and experimental design

Eight-week-old male Charles Dawley (CD) and Rowett, black hooded (BH) rats were used in the studies (Charles River, Hungary). After arrival the animals were allowed 1 week for acclimatization. All animals were maintained under standardized (light on 08:00–20:00 h; 40–70% relative humidity, 22~~ ± ~~±1°C), specified pathogen-free (SPF) conditions, with free access to water and standard rodent chow (Altromin standard diet, Germany).

We performed the following three experiments:

1. Renal functional and morphological experiment in DXR-induced acute renal failure;
2. Long term survival study with low dose DXR;
3. Short term survival study with high dose DXR.

In the functional and morphological experiment (exp. ~~1) 8 weeks old BH and CD~~1) rats (n=8/group) were intravenously injected with 5 mg/kg body weight DXR (Sicor S.r.l. Società Italiana Corticosteroidi, Italy) dissolved in saline. Equal volume of saline was administered to control animals. DXR dose was based on literature data and pilot experiments. In the pilot experiments 2 mg/kg DXR did not induce renal damage, whereas 8 mg/kg DXR caused premature moribund state in some animals.

Urinary protein and NGAL excretion was followed for 8 weeks when the experiment was terminated and renal morphology was investigated~~ 8 weeks after the DXR administration.~~. Long-term survival (exp. 2) was evaluated in ~~two groups of~~ age matched BH and CD rats (n=8/group) ~~treated similarly to the animals in the functional experiment (8 week old, (~~5 mg/kg DXR, iv~~.). Short~~). For short-term survival (exp. 3) ~~was observed in separate cohorts injected with~~ 10 mg/kg DXR was injected iv~~.~~ (n=8/group). In survival experiments animals were euthanized upon signs of uremia, which included reduced locomotion, pilo-erection, body weight loss or dyspnoea. Blood urea was > 250 mg/dl in each euthanized animal demonstrating that uremia was the cause of the moribund state.

In order to investigate whether the difference in the degree of tubulointerstitial fibrosis between the two rat strains was the consequence of different tubular protein load, or BH rats were resistant to tubulointerstitial fibrosis per se, we formed two sub-groups. In this analysis CD and BH rats treated with DXR (CD/DXRp, n=4 and BH/DXRp, n=5) were matched for urinary protein excretion and sensitive molecular, inflammatory and fibrosis parameters were compared.

Proteinuria and NGAL excretion

~~**Urinary protein excretion**~~

~~The severity of proteinuria~~Proteinuria was measured as a sensitive indicator of podocyte injury and progression of renal fibrosis. Urine was collected for 24 hours in diuresis cages (Techniplast, Italy) before (self-control) and biweekly after ~~the DXR administration until the eighth week. Urine samples were centrifuged at 14 000 g for 20 min at 4°C to remove sediment. The supernatants were stored at -20°C until~~

~~further analysis. Protein~~DXR administration. Urine protein concentration was assessed with a pyrogallol red colorimetric assay (Diagnosticum Ltd, Budapest, Hungary).~~ Briefly, the assay was carried out on 96 well plates (Greiner Bio-One GmbH, Germany). Four µl sample and 200 µl Reagent 1 (provided by the assay kit, Cat. No: 425051/DC) were added, mixed and incubated for 10 min at 37°C.~~ Optical density was measured at 598 nm with the SpectraMax 340 Microplate Spectrophotometer (Molecular Devices, Sunnyvale, USA).~~ Concentrations were calculated with SoftMax® Pro Software.~~

~~Urinary neutrophil gelatinase-associated lipocalin (NGAL)~~

~~NGAL protein~~Urine NGAL levels were measured with rat Lipocalin-2/NGAL DuoSet ELISA Development kit (R&D Systems, USA) as described by the manufacturer. ~~Briefly, the 96 well plates (Nunc™ GmbH & Co. KG, Langenselbold, Germany) were coated with diluted capture antibody, and the non-specific binding sites were blocked with assay diluent (1% BSA in PBS, pH 7.2 - 7.4). Adequately diluted samples (103 – 105 fold) were incubated in duplicates for 2 hours on the plate, and then the detection antibody was added. Next, Streptavidin-HRP was linked to the detection antibody followed by a short incubation with TMB Substrate (Sigma-Aldrich GmbH, Germany). A washing session (5 times with 300 µl of washing buffer) was performed between all steps until the addition of the substrate solution. The enzymatic reaction was terminated by H_2SO_4 containing stop solution.~~ Optical density was measured with Victor3™ 1420 Multilabel Counter (PerkinElmer, WALLAC Oy, Finland) at 450 nm with wavelength correction set to 544 nm. Concentrations were calculated with WorkOut (Dazdaq Ltd., England), using a four parameter logistic curve-fit.

Sacrifice and renal sample collection

In the functional and morphological study (exp. 1), rats were anesthetized with ketamine ~~CP-Pharma Handelsgesellschaft mbH, Burgdorf , Germany) and~~+ xylazine ~~cocktail (CP-Pharma Handelsgesellschaft mbH, Burgdorf, Germany)~~ 8 weeks after ~~the~~ DXR administration. ~~Rats were bled from the aorto-femoral bifurcation.~~ To prevent blood clotting, 1 ml/kg Na-EDTA (Sigma-Aldrich Corporation, Saint Louis, ~~Missouri~~MO, USA) was injected intraperitoneally. ~~The samples were centrifuged at 1500 g for 8 min at 4°C to acquire plasma for further analysis.~~Rats were bled from the aorto-femoral bifurcation. Animals were perfused through the aorta with 60 ml cold physiological saline to remove blood from the vasculature~~ and parenchymal organs such as the kidney.~~. After perfusion, the left kidney and the heart were removed and sectioned for further analysis. The heart and a third of the left kidney were fixed in 4% buffered formaldehyde and were later embedded in paraffin ~~(FFPE)~~ for basic histological and immunohistochemical analysis. The remaining two third of the left kidney cortex and medulla were separated, frozen in liquid nitrogen and stored at -80 °C for molecular studies.

Renal morphology~~ of DXR- and saline-injected rats~~

~~**Renal morphology** was assessed on periodic acid-Schiff stain (PAS) and Picro-Sirius red stained sections.~~ Glomerulosclerosis was assessed according to a modified [11,27] scoring system (scores 0–4) of El Nahas et al. [28] at x400 absolute magnification using an Olympus CX21 microscope (Olympus Optical Co. Ltd., Japan). Score 0: normal glomerulus. Score 1: thickening of the basal membrane. 2: mild (<25%), 2.5: severe segmental (>50%) and 3: diffuse hyalinosis. 4: total tuft

obliteration and collapse. The glomerular score of each animal was derived as the arithmetic mean of 100 glomeruli.

~~Tubular and interstitial~~Tubulointerstitial damage was assessed with a semi quantitative scale (magnification ×100) of percent ~~of~~ area affected by tubulointerstitial changes [21,29]. Score 0: normal tubules and interstitium, 1: brush border loss or tubular dilatation in <25% of the field of view (fv). 2: tubular atrophy, dilation and casts in < 50% ~~of~~ fv. Score 3: tubular and interstitial damage in < 75% ~~of~~ fv, 4: tubular atrophy, dilation, casts and fibrosis > 75% ~~of fv. Every PAS stained section received~~ fv. The overall score was the mean ~~score~~ of 15 fvs ~~(×100).~~ .

Inflammatory infiltration was assessed on hematoxylin-eosin stained sections~~. The severity of the inflammation was determined~~ by the percent of area infiltrated by inflammatory cells (magnification: x400). Score 0: normal glomeruli, tubules and interstitium, 1: inflammatory cells present in <25% ~~of~~ fv. 2: inflammation in < 50% ~~of~~ fv. Score 3: inflammation in < 75% ~~of~~ fv, 4: inflammation in > 75% of fv. ~~Overall~~The overall score was ~~given as~~ the mean of 120 ~~fv~~fvs.

Collagen deposition in the renal ~~interstitial fibrosis~~interstitium was demonstrated by Picro-Sirius Red staining~~. After deparaffinization and rehydration, nuclei were stained with Weigert's haematoxylin for 10 min followed by extensive washing with running water. Sections were stained with 0.1% solution of Sirius Red in saturated aqueous solution of picric acid for one hour at room temperature. Subsequently, sections were rinsed in 0.01 N HCl and were dehydrated in ascending concentrations of ethanol, cleared in xylene and mounted~~ as described previously. Fibrotic areas were quantified ~~by~~using Image J software (National Institutes of Health, Bethesda, Maryland, US).

Antibodies

~~The following antibodies were used for~~For Western blot and immunohistochemistry: 4-hydroxy-2-nonenal (HNE, mouse monoclonal, clone: HNEJ-2, JaICA, Japan), ~~nitrotyrosine (~~NT~~,~~ (mouse monoclonal, #189542, Cayman Chemical Company, Michigan, IL), fibronectin (rabbit polyclonal, Sigma-Aldrich, Budapest, Hungary), Connexin-43 (1:100, #3512, Cell Signaling, Beverly, MA) were used.

Western Blot

~~Snap frozen~~The kidney ~~tissue samples were ground upon freezing. The~~ samples were lysed in RIPA Buffer (Thermo Scientific, Rockford, IL~~) containing 1 mM phenylmethylsulfonyl fluoride (PMSF) and protease inhibitors.~~). Protein concentration was determined by the bicinchoninic acid (BCA) protein assay (Thermo Scientific, Rockford, IL). Twenty µg protein was resolved on 4-12% Criterion™ XT Bis-Tris Precast gels (BioRad, Hercules, CA) and transferred to nitrocellulose membrane to detect HNE or to Polyvinylidene Difluoride (PVDF) membrane to detect NT. ~~Membranes were blocked with Starting Block Blocking Buffer for 1 h~~ The primary NT antibody was applied at 1.3 µg/mL and the primary HNE antibody at 0.3 µg/mL~~ in blocking buffer, and kept overnight at 4°C. After washing in Tris-buffered saline (TBS) containing 0.2% Tween-20 (TBST), the~~. The secondary antibody (peroxidase conjugated goat anti-mouse, PerkinElmer, Santa Clara, CA) was applied at 0.25 µg/mL~~ concentration in blocking buffer for 1 h at room temperature. Blots were washed 3 times in TBST and once in TBS, and~~. Blots were incubated in enhanced chemiluminescence substrate, Supersignal West Pico Chemiluminescent Substrate (Thermo Scientific, Rockford, IL), and were exposed to photographic film. After

stripping membrane with Restore™ Western Blot Stripping Buffer (Thermo Scientific, Rockford, IL), as a loading control, peroxidase conjugated anti-actin (AC-15 Abcam, Cambridge, MA) was applied at 70 ng/mL concentration in blocking buffer for 1 h at room temperature.

Immunohistochemistry

Paraffin sections on Superfrost™ Ultra Plus Adhesion Slides (Thermo Fisher Scientific Inc, Waltham, ~~Massachusetts, USA) were deparaffinized and rehydrated in ethanol. Antigen unmasking was performed by heat-induced epitope retrieval in citrate buffer at pH: 6.00. Next, endogenous peroxidases were inactivated by hydrogen peroxide (3 % in PBS for 20 min). Sections were then blocked in normal goat serum at room temperature for one hour followed by overnight incubation with the primary antibody, HNE at 7.5 µg/mL final concentration or NT at 5 µg/mL final concentration in blocking buffer at 4°C in a moist chamber. Immune complexes were detected by using Vectastain ABC Kit (Vector Laboratories, Burlingame, CA) according to the manufacturer's instructions. Color development was induced by incubation with diaminobenzidine (DAB) kit (Vector Laboratories) for 4 min. Finally the sections were dehydrated in ethanol, cleared in xylene and mounted.~~

~~Fibronectin immunohistochemistry was performed on paraffin sections~~MA, USA) were deparaffinized and rehydrated in ethanol. Fibronectin immunohistochemistry was performed with rabbit polyclonal anti-fibronectin antibody (1:2000, Sigma-Aldrich, Budapest, Hungary), using the avidin–biotin method~~, as previously described~~ [30~~]~~]. HNE and NT immunohistochemistry was performed with mouse monoclonal antibody (HNE clone: HNEJ-2, JaICA, Japan; NT clone: #189542, Cayman Chemical Company, Michigan, IL). Color development was induced by incubation with

diaminobenzidine (DAB) kit (Vector Laboratories, Burlingame, CA). Pictures were taken from the stained sections for further analysis. The fibronectin stained ~~areas were~~area was quantified with Image J software~~ (National Institutes of Health, Bethesda, Maryland, US)~~.

Heart fibrosis markers

In a separate group, the hearts were removed and fixed in 4% buffered formalin and embedded similarly to the renal samples 8 weeks after 5 mg/kg DXR administration. Consecutive sections were stained with Masson's trichrome to detect collagen deposition as a sign of chronic fibrosis, and direct immunofluorescence was performed for connexin-43 (Cx43~~)~~), an early marker of cardiomyocyte damage.

~~Survival experiment:~~

~~Age matched, 8 weeks old CD and BH rats (n=8/group) were injected with 5 mg/kg or 10 mg/kg DXR for the survival experiments. Animals were euthanized upon signs of uremia, which included reduced locomotion, pilo-erection, body weight loss or dyspnoea. Blood urea was > 250 mg/dl in each euthanized animal demonstrating that uremia was the cause of the moribund state. Survival was assessed by Kaplan-Meier analysis.~~

Monitoring mRNA levels with Real-Time quantitative Polymerase Chain Reaction (RT-qPCR)

RNA preparation

Total RNA for RT-qPCR was extracted by homogenizing 50-80 mg pieces of renal cortex in TRI Reagent® (Molecular Research Center Inc., Cat. NO.: TR118) according to the manufacturer's protocol. ~~Briefly, RNA was precipitated by chloroform and isopropyl alcohol. The RNA pellet was washed twice with 75% ethanol, resolved in RNase free water (Lonza Group Ltd, Basel, Switzerland) and stored at -80 °C.~~ DNA contamination was removed by TURBO DNase (Life technologies, Ambion®, Cat. No: AM2238). ~~DNase activity was terminated by adding 50 µl phenol-chloroform-isoamylalcohol to 50 µl of DNase-digested RNA solution.~~ RNA concentration and purity of the samples was measured with the NanoDrop 2000c Spectrophotometer (Thermo Fisher Scientific Inc, Waltham, MA, USA). The RNA integrity was verified by electrophoretic separation on 1% agarose gel.

RT-qPCR analysis of renal mRNA levels

Reverse transcription of 1 µg total renal RNA into cDNA was carried out using random hexamer primers and the High-Capacity cDNA Archive Kit (Applied Biosystem™, USA) according to the manufacturer's protocol. ~~Briefly, 1 µg total renal RNA was denatured (70°C for 5 min), and annealed with random hexamer primers on the RNA template (25°C for 10 min). The cDNA was synthesized (37°C for 2 hours) and the reaction was terminated by heat inactivation (85°C for 2 min).~~ Messenger RNA levels of NADPH oxidase-2 (NOX-2, p91^{phox}, cytochrome b-245 beta polypeptide ~~(Cybb)),~~), neutrophil cytosolic factor 1 (Ncf1, p47^{phox}), collagen type I, alpha 1 (COL1A1), transforming growth factor β1 (TGF-β1), connective tissue growth factor (CTGF) and macrophage chemotactic protein 1, (MCP-1, chemokine (C-C motif) ligand 2, Ccl2) were measured by RT-qPCR (Qiagen, Hilden, Germany) and target mRNA levels were normalized to actin mRNA levels (Table 1).

Nephrin mRNA levels were measured by double-stranded DNA (dsDNA) dye based RT-qPCR with Maxima SYBR Green RT-qPCR Master Mix (Thermo Fisher Scientific Inc., Waltham, ~~Massachusetts~~MA, USA~~)~~), and ~~evaluated with Bio-Rad CFX96 real time PCR Detection System (Bio-Rad Laboratories, Hercules, CA, USA). Nephrin~~the mRNA values were normalized to glyceraldehyde-3-phosphate dehydrogenase ~~(GAPDH).~~. Mean values are expressed as fold mRNA levels relative to the control using the formula $2^{-\Delta(\Delta Ct)}$ (Ct: cycle time, $\Delta CT = CT_{target} - CT_{normalizer}$ and $\Delta(\Delta CT) = \Delta CT_{stimulated} - \Delta CT_{control}$) [31].

Statistics~~:~~

Two-way ANOVA with or without repeated measures were used for multiple comparisons. Post hoc analyses were done with Holm-Sidak‘s test. Logarithmic transformation of data was used if Bartlett’s test indicated a significant inhomogeneity of variances. Variables of the two sub-groups within the BH/DXR and the CD/DXR groups were compared using unpaired t-test. Survival was analyzed according to the Kaplan-Meier method. The null hypothesis was rejected if $p < 0.05$. Data were expressed as means ±SEM if not specified otherwise. All statistical analysis was done with GraphPad Prism (version 6.01, GraphPad Software Inc, San Diego, CA, USA).

Results

Heart toxicity was absent 8 weeks after 5 mg/kg DXR

~~Although DXR has been used as a toxic cardiomyopathy model, in the present study signs~~Histology of ~~cardiac toxicity were absent. In~~ the heart ~~cross-sections stained with Masson's trichrome the intensity of collagen staining was similarly mild in DXR-~~ did not show necrosis or ~~saline-injected rats. No~~other morphological ~~alteration or necrosis~~ alterations of cardiomyocytes. Massons's trichrom staining was devoid of collagen deposition, and ~~no inflammatory infiltration in the heart was observed (Figure 1/A,B). Similarly,~~ connexin-43 immunostaining ~~for connexin-43 did not differ between DXR- and saline- injected, negative control rats (Figure 1/C,D), demonstrating that~~did not demonstrate any sign of cardiomyocyte damage. Thus, a single dose of 5 mg/kg DXR did not induce any detectable chronic heart damage ~~detectable by histology or disruption of Cx43 junctional staining.~~(data not shown).

CD rats became moribund earlier than BH rats at both low and high ~~dose~~doses of DXR

BH rats became moribund significantly later following the 5 mg/kg DXR dose, compared to CD rats (Figure 1/~~E~~A). The first CD rat became moribund 75 days after ~~the~~ DXR administration, and there were no survivors after day 90 from this strain. The first BH became moribund 86 days after DXR, and there were survivors even 159 days after ~~the~~ DXR administration. The median survival after DXR was 85.5 days for the CD rats, while it was 100 days for the BH rats ($p<0.05$).

A higher dose of 10 mg/kg DXR led to a more severe outcome. The median survival of CD rats was 10 days compared to 15 days of the BH rats (Figure 1/F). DXR administration caused less severe kidney damage than subtotal nephrectomy (SNX) and salt + protein loading in our previous study [11] as demonstrated by longer survival.

DXR inhibited bodyweight gain more in CD than in BH rats

DXR-administration inhibited weight gain in BH and CD rats (Figure 2/A). BH rats had a slower growth rate than age matched CD rats. Bodyweight constantly increased in all control animals. Body weight gain was significantly inhibited in DXR-injected CD rats (CD/DXR) already starting at week 4 while CD/DXR rats started to ~~loose~~lose weight by week 8. On the contrary, significant weight gain inhibition was observed in BH rats (BH/DXR) only at week 8.

Proteinuria was milder in BH than CD rats after DXR

Proteinuria was assessed as a marker of podocyte damage and progression of renal fibrosis. In the functional and morphological experiment (exp. 1) 5 mg/kg DXR induced progressive proteinuria commencing 2 weeks after DXR in CD rats (Figure 2/B). Proteinuria started later and progressed slower in BH than in CD rats, and proteinuria was significantly milder at each time-point in BH/DXR than in CD/DXR rats.

Urinary NGAL excretion - a known marker of tubular epithelial damage - increased in both DXR-injected groups after the fourth week. Similarly to proteinuria, NGAL

excretion was significantly milder in the BH/DXR than in the CD/DXR group (Figure 2/C).

Renal histological damage and inflammation were more severe in CD than in BH rats 8 weeks after DXR

Both CD and BH rats injected with saline had normal kidneys with no or minimal glomerular and tubular abnormalities 8 weeks after the injection. DXR administration caused glomerular damage in all age-matched rats. However, BH/DXR rats had milder glomerular and tubular damage compared to CD/DXR rats (Figure 3/A-F, Table 2). Glomerular and tubular damage were distributed unevenly in rats, similarly to human focal segmental glomerulosclerosis (FSGS) [18]. In parallel with milder proteinuria and urinary excretion of NGAL in BH rats, intact glomeruli (Score: 0) were significantly more common in DXR-injected BH than in CD rats (Table 2). However, mild (Score: 0.5-1.5) (CD: 50.7 vs. BH: 28.4 %) and severe (Score ≥ 2) (CD: 13~~,~~.3 vs. BH: 3.3 %) glomerular damage was significantly more common in CD/DXR vs. BH/DXR rats. Probably as a consequence of different degrees of glomerular damage, tubulointerstitial damage was milder in BH than in CD rats (Table 2).

Eight weeks after ~~the~~ DXR administration severe inflammatory infiltration by neutrophil granulocytes, lymphocytes and macrophages was evident in the kidney samples of DXR-injected CD rats. In parallel with less proteinuria and morphological damage, inflammation was significantly milder in BH~~-~~/DXR rats than in CD rats (Figure 3/G-I).

Milder fibrosis was associated with less oxidative stress and inflammation

Fibrosis was strikingly more intense in CD/DXR than in BH/DXR rats as demonstrated by Sirius red staining (Figure 3/J,K). ~~Fibronectin, an extracellular matrix glycoprotein accumulates during fibrosis.~~ Fibronectin immunostaining was detected only in 5.2 ~~± ±~~0.6 % of the scanned areas in the saline-injected control groups, but increased significantly in the DXR-injected CD group. Significantly less fibronectin staining was detected in BH/DXR than in CD/DXR rats (Figure 3/L,M).

TGF-β1 and CTGF mRNA levels in the kidney cortex were not significantly different in the control groups compared to DXR-injected BH rats, but were significantly elevated in the CD/DXR group (Figure 4/A,B). COL1A1 mRNA levels were elevated in DXR-injected rats, but the elevation was significantly higher in the CD/DXR group than in the BH/DXR group (Figure 4/C).

Nephrin is an important component of the podocyte foot processes forming the slit diaphragm. It plays an important role in the maintenance of the structural integrity and the functional soundness of the slit diaphragm [32]. Nephrin mRNA levels decreased in the kidney cortex of the CD/DXR group, but it was not reduced in the BH/DXR group (Figure 4/D) supporting further a milder glomerular damage in BH/DXR rats.

The mRNA levels of pro-inflammatory monocyte chemotactic protein 1 (MCP-1) (Figure 4/E) and pro-oxidant markers: p91^{phox} and p47^{phox} (Figure 4/F,G) increased in both DXR-injected groups; however the elevation was milder in the BH/DXR group.

4-hydroxy-2-nonenal and nitrotyrosine

In the background of more severe kidney function deterioration demonstrated by proteinuria and fibrosis markers, severe lipid peroxidation and nitrative stress were detected in the kidneys of DXR-injected CD rats, while very mild changes were seen in the HNE or NT stained paraffin sections from the BH/DXR rats. Less staining was corroborated by Western blot demonstrating significantly more HNE and NT in CD than in BH rats 8 weeks after DXR administration (Figure 5).

Tubulointerstitial fibrosis and inflammation were milder in DXR-treated BH vs. CD rats despite similar proteinuria

Urinary protein excretion and renal nephrin mRNA levels were similar in the two subgroups of CD and BH rats (BH/DXRp, CD/DXRp) with similar proteinuria (Table 3). Markers of fibrosis such as sirius red staining and relative renal expression of TGF-β1, CTGF, COL1A1 were significantly lower in BH/DXRp vs. CD/DXRp rats. Paralleling less fibrosis, tubular damage detected by urinary NGAL excretion, markers of oxidative damage such as p47^{phox} and p91^{phox} expression and inflammation (MCP-1 expression) were significantly lower in BH/DXRp than CD/DXRp rats (Table 3).

Discussion

Renal fibrosis is an intractable medical condition with high mortality and low quality of life. We present here an animal model useful to investigate the pathomechanisms of hereditary susceptibility or resistance to renal fibrosis in various kidney injury models [10,33,34]. We demonstrated recently that BH rats were resistant to renal fibrosis with better preserved renal function and glomerular structure in a clinically relevant model of subtotal nephrectomy combined with salt and protein loading [11]. In the present study we demonstrate that less oxidative/nitrative stress and inflammation ~~were~~was associated with slower progression of fibrosis in the resistant strain. Taken together with our previous report demonstrating similar resistance of BH vs. CD rats in the subtotal nephrectomy model, our present findings underline the pathophysiological relevance of inflammation and oxidative/nitrative stress pathways in fibrosis progression.

DXR~~-~~ nephropathy in rodents is a widely used experimental model of human ~~focal segmental glomerulosclerosis (~~FSGS~~)~~ [12,35]. Direct exposure of the kidneys to DXR is a requirement for the development of podocyte injury in rats, as clipping the renal artery during DXR injection prevents nephropathy [35]. A single intravenous injection with 4-7,5 mg/kg DXR led to well predictable deterioration of glomerular structure, proteinuria, tubular and interstitial inflammation culminating in renal fibrosis in fibrosis-sensitive Sprague Dawley or Wistar rats [36]. Glomerular structural changes develop in a well predictable manner: altered mRNA levels of nephrin, podocyn and NEPH1, and swelling of the foot-processes are present at day 7 [37~~], podocyte~~]. Podocyte swelling with cytoplasmic vesicles appear at day 14, and finally widespread podocyte foot process fusion at day 28 [38]. As a marker of glomerular filtration

barrier damage, proteinuria develops [39]. Repeated low dose DXR has been widely used to induce toxic cardiomyopathy. In our model ~~of a single DXR injection,~~ cardiac toxicity was absent after a single DXR injection, as demonstrated by histology or the sensitive cardiomyopathy marker~~:~~ Cx-43.

BH rats have a slower growth rate than age matched CD rats under healthy circumstances. The body weight curve in control animals of our study were similar to ~~these~~the previous findings [40,41~~] .~~].

In our study, sensitive CD rats developed significant and progressive proteinuria starting two weeks after 5 mg/kg DXR similarly to that shown in previous publications [37-42]. Nephrin plays an important role in maintaining the structural integrity and the functional soundness of the slit diaphragm [32]. In the background of the proteinuria significant nephrin loss was demonstrated in CD rats. The severity of proteinuria was milder and progression was slower in BH rats. ~~Nephrin plays an important role in maintaining the structural integrity and the functional soundness of the slit diaphragm [32].~~ Thus, as BH rats had similar nephrin mRNA levels to the strain-identical controls, nephrin might play a central role in the progression of DXR-induced fibrosis. Proteinuria~~-~~-associated interstitial fibrosis and tubular atrophy (IFTA) has been recognized previously [43]. Podocyte dysfunction and consequent proteinuria has been recently reinforced as a major determinant of tubular injury, inflammation and apoptosis leading to progressive IFTA [44]. According to our present study and previous literature [45] IFTA developed as part of ~~the~~ DXR~~-~~ nephropathy. Urinary NGAL excretion is a sensitive marker of tubular damage not only during acute kidney injury [46,47,] but also during IFTA [48]. In our study, significantly less proteinuria was accompanied ~~with~~by reduced tubular damage and less urinary NGAL excretion after DXR in the BH than in the CD strain. Similarly, less renal damage and less

proteinuria was accompanied by better ~~preserved~~maintained body weight~~ gain~~ and significantly prolonged survival in BH rats. These data support that IFTA is secondary to proteinuria in the DXR model.

~~The primary insult to glomeruli by the~~The single administration of DXR and consequent albuminuria ~~and tubular damage culminated in glomerular sclerosis,~~led to tubulointerstitial inflammation and fibrosis demonstrated by PAS, Sirius red and ~~Fibronectin-specific staining,~~fibronectin and collagen synthesis and the presence of the pro-fibrotic transforming growth factor (TGF-β1) [49,50,] and its downstream mediator connective tissue growth factor ~~β~~ (CTGF) [51]. Significant reduction of these fibrotic pathways in the resistant BH strain underlines the relevance of the TGF-β1-CTGF cascade-mediated matrix deposition in the development of DXR-induced renal fibrosis (Figure 6).

Oxidative and nitrative stress has been proposed as the mechanism by which DXR induces glomerular toxicity in rats. Redox cycling of the ~~Quinone~~quinone functional group of DXR was proposed as the key factor ~~mediating~~in DXR nephrotoxicity [52]. Reactive oxygen species (ROS) may initiate a degenerative cascade by the oxidation of cellular thiols and lipid membrane structures [53]. DXR has been suggested to upregulate ~~the~~ NADPH-oxidase (NOX), an important source of ROS in the kidney [54]. However, the role of oxidative mechanisms in DXR toxicity has been questioned as well [55]. In our study, signs of lipid peroxidation and nitrative stress were milder in the BH rats, compared to the CD rats suggesting that less oxidative and nitrative stress may be responsible, at least in part, for the resistance of BH rats against renal fibrosis. This observation supports the role of oxidative and nitrative mechanisms in DXR toxicity.

Our results obtained in the subgroups of DXR-treated CD and BH rats with similar urinary protein excretion support our view that BH rats are less susceptible to tubulointerstital fibrosis induced by proteinuria. Renal nephrin mRNA expression was similar in the two subgroups, suggesting that the degree of podocyte injury and slit diaphragm leakiness is a primary determinant of proteinuria independent of the genetic background. However, despite similar proteinuria, most markers of renal fibrosis and inflammatory infiltration were significantly lower in BH rats. These results support the role of inflammation in proteinuria-induced tubulointerstitial fibrosis.

Resistance mechanisms against DXR nephropathy were studied previously in rat [56] and mouse [57] strains. In spontaneously hypertensive (SHR) rats, cardio- and nephrotoxicity of DXR was more severe~~,~~ than in congenic Wistar-Kyoto (WKY) and in SHR-heart failure ~~(SHHF) rats. In this study,~~ rats after subsequent administration of 2 mg/kg DXR ~~was given~~ on 8 consecutive days. ~~Renal lesions, 12~~ Twelve weeks after the last dose of DXR renal lesions were similar to those in our study with podocyte adhesion leading to glomerulosclerosis and mononuclear infiltration, tubular atrophy and fibrotic matrix expansion in the tubulointerstitium~~.~~ [56]. Severity of these histological changes correlated with strain sensitivity. Similarly to our study, strain differences were partially explained by ~~differential inflammatory response in~~a difference in the severity of inflammation and arachidonic acid metabolism.

~~The susceptibility of BALB/c mice against~~ Sensitivity to DXR nephropathy was ~~associated with a gene involved~~investigated previously in ~~DXR detoxification. In this study C57BL/6 mice - generally~~ fibrosis-resistant ~~to renal fibrosis - were compared to~~ C57BL/6 and -sensitive ~~Balb/c mice with known differences in inflammatory response. C57Bl/6 mice are typically Th1 predominant, vs. Th2 predominance in~~ BALB/c mice [10~~As fibrosis is mediated by myofibroblasts activated by TGF-β1,~~

~~MCP-1, etc. [59], Th2 predominance may favor fibrotic processes, whereas Th1 predominance could be responsible for renal fibrosis resistance of Bl/6 mice.~~]. The difference in susceptibility was attributed to a mutation in the PRKDC gene encoding the **c**atalytic subunit of a DNA activated protein kinase (DNA-PK), a double stranded break repair protein [10,58]. This mutation is also responsible for the severe combined immunodeficiency (SCID) phenotype in mice and rats [59]. DNA-PK expression and activity was also profoundly lower in BALB/c than C57BL/6 mice in a radiation induced apoptosis model [60]. Thus, DNA-PK seems to be crucial in toxic injury models. As inflammation and related oxidative stress also induces DNA damage, the PRKDC gene may play an important role also in our model.

Fibrosis is mediated by myofibroblasts activated by TGF-β1, MCP-1, etc. [61]. In our study, decreased MCP-1 mRNA levels were found in resistant BH rats, which is one of the key chemokines for the migration and infiltration of macrophages to sites of inflammation [62]. The mRNA levels of p91^{phox}, also known as NADPH oxidase 2 (NOX2) ~~was also~~ were also lower in BH rats. NOX2 plays an important role in ROS production of phagocytes and T cells. Furthermore, the mRNA ~~levels~~level of p47^{phox}, which plays a role in the activation of the NOX2/p22^{phox} complex in the membrane of phagocytes [63], was also milder in BH rats. These findings suggest that less inflammation, accompanied by milder ROS production of the neutrophil cells and macrophages may play a role in the resistance of BH rats against DXR nephropathy.

Conclusions:

In conclusion, resistance of BH rats against renal fibrosis highlighted the role of inflammation-induced oxidative/nitrative stress in chronic podocyte injury leading to

glomerulosclerosis and consequent proteinuria in DXR nephropathy. Tubulointerstitial fibrosis is most likely secondary to proteinuria in this model.

Acknowledgements

Support was provided to P. Hamar from the Hungarian Research Fund: OTKA-ANN(FWF) 110810 and OTKA-SNN 114619, and to P. Pacher from the Intramural Research Program of NIAAA/NIH. P Hamar acknowledges support from the Bolyai Research Scholarship of the Hungarian Academy of Sciences and the Merit Prize of the Semmelweis University.

We wish to thank Róbert Glávits, DVM, PhD, DSc for his help in the histological assessment of the kidney samples.

References

1. Comas J, Arcos E, Castell C, Cases A, Martinez-Castelao A, et al. (2013) Evolution of the incidence of chronic kidney disease Stage 5 requiring renal replacement therapy in the diabetic population of Catalonia. Nephrol Dial Transplant 28: 1191-1198.
2. (2014) National Chronic Kidney Disease Fact Sheet. Available: http://wwwcdcgov/diabetes/pubs/factsheets/kidneyhtm Accessed 3 August 2014.
3. Boor P, Floege J (2011) Chronic kidney disease growth factors in renal fibrosis. Clin Exp Pharmacol Physiol 38: 441-450.
4. Hostetter TH, Olson JL, Rennke HG, Venkatachalam MA, Brenner BM (2001) Hyperfiltration in remnant nephrons: a potentially adverse response to renal ablation. J Am Soc Nephrol 12: 1315-1325.
5. Cameron JS (1996) The enigma of focal segmental glomerulosclerosis. Kidney Int Suppl 57: S119-131.
6. Fitzgibbon WR, Greene EL, Grewal JS, Hutchison FN, Self SE, et al. (1999) Resistance to remnant nephropathy in the Wistar-Furth rat. J Am Soc Nephrol 10: 814-821.
7. Fleck C, Appenroth D, Jonas P, Koch M, Kundt G, et al. (2006) Suitability of 5/6 nephrectomy (5/6NX) for the induction of interstitial renal fibrosis in rats--influence of sex, strain, and surgical procedure. Exp Toxicol Pathol 57: 195-205.
8. Rostand SG, Kirk KA, Rutsky EA, Pate BA (1982) Racial differences in the incidence of treatment for end-stage renal disease. N Engl J Med 306: 1276-1279.
9. Kaplan JM, Kim SH, North KN, Rennke H, Correia LA, et al. (2000) Mutations in ACTN4, encoding alpha-actinin-4, cause familial focal segmental glomerulosclerosis. Nat Genet 24: 251-256.
10. Papeta N, Chan KT, Prakash S, Martino J, Kiryluk K, et al. (2009) Susceptibility loci for murine HIV-associated nephropathy encode trans-regulators of podocyte gene expression. J Clin Invest 119: 1178-1188.
11. Kokeny G, Nemeth Z, Godo M, Hamar P (2010) The Rowett rat strain is resistant to renal fibrosis. Nephrol Dial Transplant 25: 1458-1462.
12. Lee VW, Harris DC (2011) Adriamycin nephropathy: a model of focal segmental glomerulosclerosis. Nephrology (Carlton) 16: 30-38.
13. Zhu C, Xuan X, Che R, Ding G, Zhao M, et al. (2014) Dysfunction of the PGC-1alpha-mitochondria axis confers adriamycin-induced podocyte injury. Am J Physiol Renal Physiol 306: F1410-1417.
14. Tapia E, Soto V, Ortiz-Vega KM, Zarco-Marquez G, Molina-Jijon E, et al. (2012) Curcumin induces Nrf2 nuclear translocation and prevents glomerular hypertension, hyperfiltration, oxidant stress, and the decrease in antioxidant enzymes in 5/6 nephrectomized rats. Oxid Med Cell Longev 2012: 269039.
15. Toba H, Nakashima K, Oshima Y, Kojima Y, Tojo C, et al. (2010) Erythropoietin prevents vascular inflammation and oxidative stress in subtotal nephrectomized rat aorta beyond haematopoiesis. Clin Exp Pharmacol Physiol 37: 1139-1146.
16. Rashid S, Ali N, Nafees S, Ahmad ST, Arjumand W, et al. (2013) Alleviation of doxorubicin-induced nephrotoxicity and hepatotoxicity by chrysin in Wistar rats. Toxicol Mech Methods 23: 337-345.
17. Park EJ, Kwon HK, Choi YM, Shin HJ, Choi S (2012) Doxorubicin induces cytotoxicity through upregulation of pERK-dependent ATF3. PLoS One 7: e44990.
18. Ma H, Wu Y, Zhang W, Dai Y, Li F, et al. (2013) The effect of mesenchymal stromal cells on doxorubicin-induced nephropathy in rats. Cytotherapy 15: 703-711.

666 19. Polhill T, Zhang GY, Hu M, Sawyer A, Zhou JJ, et al. (2012) IL-2/IL-2Ab complexes induce
667 regulatory T cell expansion and protect against proteinuric CKD. J Am Soc Nephrol 23: 1303-
668 1308.
669 20. Takimoto CC, E. (2008) "Principles of Oncologic Pharmacotherapy". In: Pazdur R, Camphausen KA,
670 Wagman LD, Hoskins WJ, editors. Cancer Management: A Multidisciplinary Approach. 11. ed
671 ed: Cmp United Business Media.
672 21. Fujimura T, Yamagishi S, Ueda S, Fukami K, Shibata R, et al. (2009) Administration of pigment
673 epithelium-derived factor (PEDF) reduces proteinuria by suppressing decreased nephrin and
674 increased VEGF expression in the glomeruli of adriamycin-injected rats. Nephrol Dial
675 Transplant 24: 1397-1406.
676 22. Ramadan R, Faour D, Awad H, Khateeb E, Cohen R, et al. (2012) Early treatment with everolimus
677 exerts nephroprotective effect in rats with adriamycin-induced nephrotic syndrome. Nephrol
678 Dial Transplant 27: 2231-2241.
679 23. Deman A, Ceyssens B, Pauwels M, Zhang J, Houte KV, et al. (2001) Altered antioxidant defence in
680 a mouse adriamycin model of glomerulosclerosis. Nephrol Dial Transplant 16: 147-150.
681 24. Wu H, Wang Y, Tay YC, Zheng G, Zhang C, et al. (2005) DNA vaccination with naked DNA encoding
682 MCP-1 and RANTES protects against renal injury in adriamycin nephropathy. Kidney Int 67:
683 2178-2186.
684 25. Mahajan D, Wang Y, Qin X, Wang Y, Zheng G, et al. (2006) CD4+CD25+ regulatory T cells protect
685 against injury in an innate murine model of chronic kidney disease. J Am Soc Nephrol 17:
686 2731-2741.
687 26. Liu S, Jia Z, Zhou L, Liu Y, Ling H, et al. (2013) Nitro-oleic acid protects against adriamycin-induced
688 nephropathy in mice. Am J Physiol Renal Physiol 305: F1533-1541.
689 27. Hamar P, Liptak P, Heemann U, Ivanyi B (2005) Ultrastructural analysis of the Fisher to Lewis rat
690 model of chronic allograft nephropathy. Transpl Int 18: 863-870.
691 28. el Nahas AM, Zoob SN, Evans DJ, Rees AJ (1987) Chronic renal failure after nephrotoxic nephritis
692 in rats: contributions to progression. Kidney Int 32: 173-180.
693 29. Hamar P, Kokeny G, Liptak P, Krtil J, Adamczak M, et al. (2007) The combination of ACE inhibition
694 plus sympathetic denervation is superior to ACE inhibitor monotherapy in the rat renal
695 ablation model. Nephron Exp Nephrol 105: e124-136.
696 30. Fang L, Radovits T, Szabo G, Mozes MM, Rosivall L, et al. (2013) Selective phosphodiesterase-5
697 (PDE-5) inhibitor vardenafil ameliorates renal damage in type 1 diabetic rats by restoring
698 cyclic 3',5' guanosine monophosphate (cGMP) level in podocytes. Nephrol Dial Transplant 28:
699 1751-1761.
700 31. Livak KJ, Schmittgen TD (2001) Analysis of relative gene expression data using real-time
701 quantitative PCR and the 2(-Delta Delta C(T)) Method. Methods 25: 402-408.
702 32. Machado JR, Rocha LP, Neves PD, Cobo Ede C, Silva MV, et al. (2012) An overview of molecular
703 mechanism of nephrotic syndrome. Int J Nephrol 2012: 937623.
704 33. Chua S, Jr., Li Y, Liu SM, Liu R, Chan KT, et al. (2010) A susceptibility gene for kidney disease in an
705 obese mouse model of type II diabetes maps to chromosome 8. Kidney Int 78: 453-462.
706 34. Zheng Z, Pavlidis P, Chua S, D'Agati VD, Gharavi AG (2006) An ancestral haplotype defines
707 susceptibility to doxorubicin nephropathy in the laboratory mouse. J Am Soc Nephrol 17:
708 1796-1800.
709 35. de Mik SM, Hoogduijn MJ, de Bruin RW, Dor FJ (2013) Pathophysiology and treatment of focal
710 segmental glomerulosclerosis: the role of animal models. BMC Nephrol 14: 74.
711 36. Bertani T, Rocchi G, Sacchi G, Mecca G, Remuzzi G (1986) Adriamycin-induced glomerulosclerosis
712 in the rat. Am J Kidney Dis 7: 12-19.
713 37. Otaki Y, Miyauchi N, Higa M, Takada A, Kuroda T, et al. (2008) Dissociation of NEPH1 from
714 nephrin is involved in development of a rat model of focal segmental glomerulosclerosis. Am
715 J Physiol Renal Physiol 295: F1376-1387.

716 38. Fan Q, Xing Y, Ding J, Guan N (2009) Reduction in VEGF protein and phosphorylated nephrin
717 associated with proteinuria in adriamycin nephropathy rats. Nephron Exp Nephrol 111: e92-
718 e102.
719 39. Jeansson M, Bjorck K, Tenstad O, Haraldsson B (2009) Adriamycin alters glomerular endothelium
720 to induce proteinuria. J Am Soc Nephrol 20: 114-122.
721 40. (2014) Charles River Laboratories: RNU rat. Available: http://wwwcrivercom/products-
722 services/basic-research/find-a-model/rnu-rat Accessed: 30 November 2014.
723 41. Pettersen JC, Morrissey RL, Saunders DR, Pavkov KL, Luempert LG, 3rd, et al. (1996) A 2-year
724 comparison study of Crl:CD BR and Hsd:Sprague-Dawley SD rats. Fundam Appl Toxicol 33:
725 196-211.
726 42. Zou MS, Yu J, Nie GM, He WS, Luo LM, et al. (2010) 1, 25-dihydroxyvitamin D3 decreases
727 adriamycin-induced podocyte apoptosis and loss. Int J Med Sci 7: 290-299.
728 43. Gross ML, Hanke W, Koch A, Ziebart H, Amann K, et al. (2002) Intraperitoneal protein injection in
729 the axolotl: the amphibian kidney as a novel model to study tubulointerstitial activation.
730 Kidney Int 62: 51-59.
731 44. Zoja C, Abbate M, Remuzzi G (2014) Progression of renal injury toward interstitial inflammation
732 and glomerular sclerosis is dependent on abnormal protein filtration. Nephrol Dial
733 Transplant.
734 45. Cianciolo R, Yoon L, Krull D, Stokes A, Rodriguez A, et al. (2013) Gene expression analysis and
735 urinary biomarker assays reveal activation of tubulointerstitial injury pathways in a rodent
736 model of chronic proteinuria (Doxorubicin nephropathy). Nephron Exp Nephrol 124: 1-10.
737 46. Mishra J, Ma Q, Prada A, Mitsnefes M, Zahedi K, et al. (2003) Identification of neutrophil
738 gelatinase-associated lipocalin as a novel early urinary biomarker for ischemic renal injury. J
739 Am Soc Nephrol 14: 2534-2543.
740 47. Mishra J, Dent C, Tarabishi R, Mitsnefes MM, Ma Q, et al. (2005) Neutrophil gelatinase-associated
741 lipocalin (NGAL) as a biomarker for acute renal injury after cardiac surgery. Lancet 365: 1231-
742 1238.
743 48. Entin-Meer M, Ben-Shoshan J, Maysel-Auslender S, Levy R, Goryainov P, et al. (2012) Accelerated
744 renal fibrosis in cardiorenal syndrome is associated with long-term increase in urine
745 neutrophil gelatinase-associated lipocalin levels. Am J Nephrol 36: 190-200.
746 49. Lan HY (2011) Diverse roles of TGF-beta/Smads in renal fibrosis and inflammation. Int J Biol Sci 7:
747 1056-1067.
748 50. Yanagita M (2012) Inhibitors/antagonists of TGF-beta system in kidney fibrosis. Nephrol Dial
749 Transplant 27: 3686-3691.
750 51. Ruster C, Wolf G (2011) Angiotensin II as a morphogenic cytokine stimulating renal fibrogenesis. J
751 Am Soc Nephrol 22: 1189-1199.
752 52. Fukuda F, Kitada M, Horie T, Awazu S (1992) Evaluation of adriamycin-induced lipid peroxidation.
753 Biochem Pharmacol 44: 755-760.
754 53. Qin XJ, He W, Hai CX, Liang X, Liu R (2008) Protection of multiple antioxidants Chinese herbal
755 medicine on the oxidative stress induced by adriamycin chemotherapy. J Appl Toxicol 28:
756 271-282.
757 54. Guo J, Ananthakrishnan R, Qu W, Lu Y, Reiniger N, et al. (2008) RAGE mediates podocyte injury in
758 adriamycin-induced glomerulosclerosis. J Am Soc Nephrol 19: 961-972.
759 55. Morgan WA, Kaler B, Bach PH (1998) The role of reactive oxygen species in adriamycin and
760 menadione-induced glomerular toxicity. Toxicol Lett 94: 209-215.
761 56. Sharkey LC, Radin MJ, Heller L, Rogers LK, Tobias A, et al. (2013) Differential cardiotoxicity in
762 response to chronic doxorubicin treatment in male spontaneous hypertension-heart failure
763 (SHHF), spontaneously hypertensive (SHR), and Wistar Kyoto (WKY) rats. Toxicol Appl
764 Pharmacol 273: 47-57.

57. Zheng Z, Schmidt-Ott KM, Chua S, Foster KA, Frankel RZ, et al. (2005) A Mendelian locus on chromosome 16 determines susceptibility to doxorubicin nephropathy in the mouse. Proc Natl Acad Sci U S A 102: 2502-2507.
58. Papeta N, Zheng Z, Schon EA, Brosel S, Altintas MM, et al. (2010) Prkdc participates in mitochondrial genome maintenance and prevents Adriamycin-induced nephropathy in mice. J Clin Invest 120: 4055-4064.
59. Mashimo T, Takizawa A, Kobayashi J, Kunihiro Y, Yoshimi K, et al. (2012) Generation and characterization of severe combined immunodeficiency rats. Cell Rep 2: 685-694.
60. Mori N, Matsumoto Y, Okumoto M, Suzuki N, Yamate J (2001) Variations in Prkdc encoding the catalytic subunit of DNA-dependent protein kinase (DNA-PKcs) and susceptibility to radiation-induced apoptosis and lymphomagenesis. Oncogene 20: 3609-3619.
61. Wynn TA (2008) Cellular and molecular mechanisms of fibrosis. J Pathol 214: 199-210.
62. Zhang Y, Bao S, Kuang Z, Ma Y, Hu Y, et al. (2014) Urotensin II promotes monocyte chemoattractant protein-1 expression in aortic adventitial fibroblasts of rat. Chin Med J (Engl) 127: 1907-1912.
63. Lee K, Won HY, Bae MA, Hong JH, Hwang ES (2011) Spontaneous and aging-dependent development of arthritis in NADPH oxidase 2 deficiency through altered differentiation of CD11b+ and Th/Treg cells. Proc Natl Acad Sci U S A 108: 9548-9553.

~~-~~Figure legends

Figure 1: ~~Myocardial morphology (A-D) and survival~~Survival (long term: ~~E~~A**,** short term: ~~F)~~

~~A,~~**B**~~: Masson's Trichrome staining (400x~~**)**

~~**C,D:** Desmin-Connexin-43 (Cx43) immunofluorescent staining (400x) 8 weeks after 5 mg/kg doxorubicin (DXR) administration.~~

~~**E,F:** Survival:~~ CD: CD rats, BH: BH rats. DXR: Doxorubicin injected rats (5 mg/kg).

Figure 2: Body weight changes (A) proteinuria (B) and urinary NGAL excretion (C)

CD: CD rats, BH: BH rats. c: saline-injected, DXR: Doxorubicin-injected rats (5 mg/kg).

*: $p<0.05$ vs. strain-identical, negative control group, †: $p<0.05$ vs. CD/DXR, positive control group.

Figure 3: Renal histopathology

Top row (periodic acid–Schiff (PAS) staining) (**A-C**): Glomerular damage in the affected areas.

Middle row ~~(periodic acid–Schiff (~~PAS~~)~~ staining) (**D-F**): Tubular damage in the affected areas.

Lower row (hematoxylin-eosin (HE) staining) (**G-I**): Tubulointerstitial inflammatory infiltration.

Saline-injected control rats (**A,D,G**); CD-DXR: doxorubicin-injected (5 mg/kg) CD rats (**B,E,H**); BH-DXR: doxorubicin-injected BH rats (**C,F,I**)

J: Sirius red staining (100x)

L: Fibronectin immunohistochemistry (400x)

K, M: computerized quantification of the immunostained areas

CD: CD rats, BH: BH rats. c: saline-injected, DXR: Doxorubicin-injected rats (5 mg/kg).

*: p<0.05 vs. strain-identical, control group, †: p<0.05 vs. CD/DXR, control group.

Figure 4: Renal cortical mRNA levels of fibrosis related, inflammatory and oxidative markers

(**A:** TGF-~~β~~β1, **B:** CTGF, **C:** COL1A1, **D:** nephrin, **E:** MCP-1 **F:** $p47^{phox}$, **G**: $p91^{phox}$

CD: CD rats, BH: BH rats. c: saline-injected, DXR: Doxorubicin-injected rats (5 mg/kg).

TGF-β1: transforming growth factor β1; CTGF: connective tissue growth factor; COL1A1: collagen type I alpha 1; MCP-1: monocyte chemotactic protein 1; $p47^{phox}$: neutrophil cytosolic factor 1; $p91^{phox}$: cytochrome b-245, beta polypeptide;

*: p<0.05 vs. strain-identical control group, †: p<0.05 vs. CD/DXR.

Figure 5: Oxidative/nitrative stress markers.

A: 4-hydroxy-2-nonenal (~~4-~~HNE) immunhistology (400x) and **B**: quantification by Western blot.

C: Nitrotyrosine (NT) immunohistology (400x) and **D:** quantification by Western blot.

CD: CD rats, BH: BH rats. c: saline-injected, DXR: Doxorubicin-injected rats (5 mg/kg).

Figure 6: Suggested mechanisms of doxorubicin induced nephropathy.

A single administration of doxorubicin induced podocyte damage demonstrated by loss of nephrin and leading to proteinuria. Proteinuria damages tubules as demonstrated by increased urinary NGAL excretion. Tubular damage leads to interstitial inflammation and fibrosis with collagen and fibronectin deposition~~, which triggers further immune activation and~~. Inflammation is accompanied by oxidative/nitrative damage triggering further immune activation. Reverse arrows symbolize main elements of the vicious circle. Sustained injury activates the TGF-β1 and CTGF profibrotic axis. Sustained injury eventually leads to fibrotic end-stage kidney.

NGAL: neutrophil gelatinase-associated lipocalin; TGF-β1: transforming growth factor β1; CTGF: connective tissue growth factor

831

Tables

Table 1: Qiagen primer reference numbers

Gene	Reference sequence	Qiagen primer reference number
~~p91-phox~~p91^{phox} (NOX2)	NM_023965.1	QT00195300
p47^{phox} (Ncf1)	NM_053734	QT00189728
MCP-1 (Ccl2)	NM_031530.1	QT00183253
TGF-β1	NM_021578.2	QT00187796
CTGF	NM_022266.2	QT00182021
COL1A1	NM_053304.1	QT02285619

Table 2: Renal morphology:

Groups	Undamaged glomeruli (%)	Glomerulosclerosis score	Tubular score	Inflammation score
CD/DXR	36.3±13.4	0.79±0.22	2.01±0.64	1.61±0.32
BH/DXR	68.3±8.4	0.32±0.11	0.86±0.44	1.06±0.20
Control	93.3±4.4	0.06±0.04	0.00±0.00	0.18±0.06
P value (CD/DXR vs. BH/DXR)	<0.001	<0.001	<0.001	<0.01

CD: CD rats, BH: BH rats. Control: saline-injected, DXR: Doxorubicin-injected rats (5 mg/kg).

Mean±SD, n=10/group.

Table 3: Comparison of BH/DXRp and CD/DXRp subgroups:

	CD/DXRp (n=4)	BH/DXRp (n=5)	P value
U Protein, week 8 (mg/24h)	396.5±82.2	362.5±30.3	0.42
Nephrin	0.68±0.16	0.87±0.19	0.19
U NGAL, week 8 (mg/24h)	10.1±2.0	5.2±1.6	**<0.01**
Sirius red (%)	18.0±1.6	11.8±1.0	**<0.01**
Fibronectin (%)	7.91±2.45	5.55±1.19	0.16
TGF-β1	6.00±2.36	2.13±1.23	**<0.05**
CTGF	3.71±2.10	0.54±0.11	**<0.05**
COL1A1	23.09±6.14	5.79±2.41	**<0.01**
$p47^{phox}$	4.69±1.51	1.95±0.36	**<0.05**
$p91^{phox}$	10.69±2.47	1.94±0.78	**<0.01**
MCP-1	9.23 3.28	3.46±0.99	**<0.05**